19. Fulp, C.T., Cho, G., Marsh, E.D., Nasrallah, I.M., Labosky, P.A. and Golden, J.A. (2008) Identification of Arx transcriptional targets in the developing basal forebrain. *Hum. Mol. Genet.*, **17**, 3740–3760.
20. Colasante, G., Collombat, P., Raimondi, V., Bonanomi, D., Ferrai, C., Maira, M., Yoshikawa, K., Mansouri, A., Valtorta, F., Rubenstein, J.L. and Broccoli, V. (2008) Arx is a direct target of Dlx2 and thereby contributes to the tangential migration of GABAergic interneurons. *J Neurosci.*, **28**, 10674–10686.
21. Tamamaki, N., Yanagawa, Y., Tomioka, R., Miyazaki, J., Obata, K. and Knaeko, T. (2003) Green fluorescent protein expression and colocalization with calretinin, paralbumin, and somatostain in the GSAD67-GFP knock-in mouse. *J. Comp. Neurol.*, **467**, 60–79.
22. Tanaka, D.H., Maekawa, K., Yanagawa, Y., Obata, K. and Murakami, F. (2006) Multidirectional and multizonal migration of GABAergic interneurons in the developing cerebral cortex. *Development*, **133**, 2167–2176.
23. Hevner, R.F., Shi, L., Justice, N., Hsueh, Y.-P., Sheng, M., Smiga, S., Bulfone, A., Goffinet, A.M., Campagnoni, A.T. and Rubenstein, J.L.R. (2001) Tbr1 regulates differentiation of the preplate and layer 6. *Neuron*, **29**, 353–366.
24. Ferland, R.J., Cherry, T.J., Preware, P.O., Morrisey, E.E. and Walsh, C.A. (2003) Characterization of Foxp2 and Foxp1 mRNA and protein in the developing and mature brain. *J. Comp. Neurol.*, **460**, 266–279.
25. Britanova, O., Romero, C.J., Cheung, A., Kwan, K.Y., Schwark, M., Gyorgy, A., Vogel, T., Akopov, S., Mitkovski, M., Agoston, D. *et al.* (2008) Satb2 is a postmitotic determinant for upper-layer neuron specification in the neocortex. *Neuron*, **57**, 378–392.
26. Bonneau, D., Toutain, A., Laguerriere, A., Marret, S., Saugier-Veber, P., Barthez, M.A., Radi, S., Biran-Mucignat, V., Rodriguez, D. and Gélot, A. (2002) X-linked lissencephaly with absent corpus callosum and ambiguous genitalia (XLAG): clinical, magnetic resonance imaging, and neuropathological findings. *Ann. Neurol.*, **51**, 340–349.
27. Okazaki, S., Ohsawa, M., Kuki, I., Kawasaki, H., Koriyama, T., Ri, S., Ichiba, H., Hai, E., Inoue, T., Nakamura, H. *et al.* (2008) *Aristaless*-related homeobox gene disruption leads to abnormal distribution of GABAergic interneurons in the human neocortex: evidence based on a case of X-linked lissencephaly with abnormal genitalia (XLAG). *Acta Neuropathol.*, **116**, 453–462.
28. Nasrallah, I.M., Minarcik, J.C. and Golden, J.A. (2004) A polyalanine tract expansion in ARX forms intranuclear inclusions and results in increased cell death. *J. Cell Biol.*, **167**, 411–416.
29. Shoubridge, C., Cloosterman, D., Parkinson-Lawerence, E., Brooks, D. and Gecz, J. (2007) Molecular pathology of expanded polyalanine tract mutations in the *Aristaless*-related homeobox gene. *Genomics*, **90**, 59–71.
30. Forman, M.S., Squier, W., Dobyns, W.B. and Golden, J.A. (2006) Genotypically defined lissencephalies show distinct pathologies. *J. Neuropathol. Exp. Neurol.*, **64**, 847–857.
31. Friocourt, G., Kanatani, S., Tabata, H., Yozu, M., Takahashi, T., Antypa, M., Raguenes, O., Chelly, J., Ferec, C., Nakajima, K. and Parnavelas, J.G. (2008) Cell-autonomous roles of ARX in cell proliferation and neuronal migration during corticogenesis. *J. Neurosci.*, **28**, 5794–5705.
32. Wilson, D.S., Sheng, G., Jun, S. and Desplan, C. (1996) Conservation and diversification in homeodomain-DNA interactions: a comparative genetic analysis. *Proc. Natl Acad. Sci. USA*, **93**, 6886–6891.
33. Lacey, J.C. Jr and Pruitt, K.M. (1996) Origin of the genetic code. *Nature*, **223**, 799–804.
34. Powell, E.M., Campbell, D.B., Stanwood, G.D., Davis, C., Noebels, J.L. and Levitt, P. (2003) Genetic disruption of cortical interneuron development causes region- and GABA cell type-specific deficits, epilepsy, and behavioral dysfunction. *J. Neurosci.*, **23**, 622–631.
35. Cobos, I., Elisa, M., Calcagnotto, E., Vilaythong, A.J., Thwin, M.T., Noebel, J.L., Baraban, S.C. and Rubenstein, J.L.R. (2005) Mice lacking *Dlx1* show subtype-specific loss of interneurons, reduce inhibition and epilepsy. *Nat. Neurosci.*, **8**, 1059–1063.
36. Freund, T.F. and Antal, M. (1988) GABA-containing neurons in the septum control inhibitory interneurons in the hippocampus. *Nature*, **336**, 170–173.
37. Frotscher, M. and Léránth, C. (1985) Cholinergic innervation of the rat hippocampus as revealed by choline acetyltransferase immunocytochemistry: a combined light and electron microscopic study. *J. Comp. Neurol.*, **225**, 327–343.
38. Ferencz, I., Leanza, G., Nanobashvili, A., Kokaia, Z., Kokaia, M. and Lindvall, O. (2001) Septal cholinergic neurons suppress seizure development in hippocampal kindling in rats: comparison with noradrenergic neurons. *Neuroscience*, **102**, 819–832.
39. Butuzova, M.V. and Kitchigina, V.F. (2008) Repeated blockade of GABAA receptors in the medial septal region induces epileptiform activity in the hippocampus. *Neurosci. Lett.*, **434**, 133–138.
40. An, J.J., Bae, M.H., Cho, S.R., Lee, S.H., Choi, S.H., Lee, B.H., Shin, H.S., Kim, Y.N., Park, K.W., Borrelli, E. and Baik, J.H. (2004) Altered GABAergic neurotransmission in mice lacking dopamine D2 receptors. *Mol. Cell. Neurosci.*, **25**, 732–741.
41. Liu, Q., Han, D., Wang, S. and Zou, Z.Y. (2005) Characteristic neuronal firing interspike intervals in laterodorsal thalamic nuclei induced by tetanization of rat caudate putamen: possible relations to hippocampal electroencephalogram changes. *Acta Physiologica Sinica*, **25**, 573–586.
42. Bracci, E., Centonze, D., Bernardi, G. and Calabresi, P. (2004) Engagement of rat striatal neurons by cortical epileptiform activity investigated with paired recordings. *J. Nuerophysiol.*, **92**, 2725–2737.
43. Wu, J.F., Han, D., Hu, L. and Zou, Z.Y. (2006) Contralateral 80–280 Hz EEG ripples and hippocampal single unit discharge inhibition in response to acute tetanization of rat right caudate putamen *in vivo*. *Epilepsy Res.*, **70**, 59–72.
44. Myhrer, T. (2003) Neurotransmitter systems involved in learning and memory in the rat: a meta-analysis based on studies of four behavioral tasks. *Brain Res. Brain Res. Rev.*, **41**, 268–287.
45. McDonald, R.J. and White, N.M. (1993) A triple dissociation of memory systems: hippocampus, amygdala, and dorsal striatum. *Behav. Neurosci.*, **107**, 3–22.
46. Parent, M.B. and Baxter, M.G. (2004) Septohippocampal acetylcholine: involved in but not necessary for learning and memory? *Learn. Mem.*, **11**, 9–20.
47. Fuchs, E.C., Zivkovic, A.R., Cunningham, M.O., Middleton, S., Lebeau, F.E., Bannerman, D.M., Rozov, A., Whittington, M.A., Traub, R.D., Rawlins, J.N. and Monyer, H. (2007) Recruitment of parvalbumin-positive interneurons determines hippocampal function and associated behavior. *Neuron*, **53**, 591–604.
48. Tepper, J.M. and Bolam, J.P. (2004) Functional diversity and specificity of neostriatal interneurons. *Curr. Opin. Neurobiol.*, **14**, 685–692.
49. Kitabatake, Y., Hikida, T., Watanabe, D., Pastan, I. and Nakanishi, S. (2003) Impairment of reward-related learning by cholinergic cell ablation in the striatum. *Proc. Natl Acad. Sci. USA*, **100**, 7965–7970.
50. Ehninger, D., Li, W., Fox, K., Stryker, M.P. and Silva, A.J. (2008) Reversing neurodevelopmental disorders in adults. *Neuron*, **60**, 950–960.
51. Paxions, G. and Franklin, K.B.J. (1997) *The Mouse Brain.* Academic Press, New York.
52. Fragkouli, A., Hean, C., Errington, M., Cooke, S., Grigoriou, M., Bliss, T., Stylianopoulou, F. and Pachnis, V. (2005) Loss of forebrain cholinergic neurons and impairment in spatial leaning and memory in LHX7-deficient mice. *Eur. J. Nurosci.*, **21**, 2923–2938.
53. Karl, T., Pabst, R. and von Hörsten, S. (2003) Behavioral phenotyping of mice in pharmacological and toxicological research. *Exp. Toxicol. Pathol.*, **55**, 69–83.
54. Miyakawa, T., Yamada, M., Duttaroy, A. and Wess, J. (2001) Hyperactivity and intact hippocampus-dependent learning in mice lacking the M1 muscarinic acetylcholine receptor. *J. Neurosci.*, **21**, 5239–5250.
55. Robert, J.M. and Morman, N.M. (1993) A triple dissociation of memory systems: hippocampus, amygdala, and dorsal striatum. *Behav. Neuro.*, **107**, 3–32.

Mitochondrion 9 (2009) 115–122

Contents lists available at ScienceDirect

Mitochondrion

journal homepage: www.elsevier.com/locate/mito

Different effects of novel mtDNA G3242A and G3244A base changes adjacent to a common A3243G mutation in patients with mitochondrial disorders

Masakazu Mimaki [a], Hideyuki Hatakeyama [a], Takashi Ichiyama [b], Hiroshi Isumi [b], Susumu Furukawa [b], Manami Akasaka [c], Atsushi Kamei [c], Hirofumi Komaki [a], Ichizo Nishino [d], Ikuya Nonaka [e], Yu-ichi Goto [a,*]

[a] Department of Mental Retardation and Birth Defect Research, National Institute of Neuroscience, National Center of Neurology and Psychiatry (NCNP), 4-1-1 Ogawahigashi, Kodaira, Tokyo, Japan
[b] Department of Pediatrics, Yamaguchi University School of Medicine, Yamaguchi, Japan
[c] Department of Pediatrics, Iwate Medical University, Iwate, Japan
[d] Department of Neuromuscular Research, National Institute of Neuroscience, NCNP, Kodaira, Tokyo, Japan
[e] National Center Hospital for Mental, Nervous and Muscular Disorders, NCNP, Kodaira, Tokyo, Japan

ARTICLE INFO

Article history:
Received 30 July 2008
Received in revised form 9 November 2008
Accepted 12 January 2009
Available online 21 January 2009

Keywords:
Mitochondrial DNA $tRNA^{Leu(UUR)}$ gene
Mutation
Mitochondrial myopathy encephalopathy lactic acidosis and stroke-like episodes (MELAS)
Cybrid
ATP production
BN-PAGE

ABSTRACT

Two novel mitochondrial DNA base changes were identified at both sides of the 3243A > G mutation, the most common mutation associated with mitochondrial myopathy, encephalopathy, lactic acidosis, and stroke-like episodes (MELAS). One was a 3244G > A transition in a girl with MELAS. The other was a 3242G > A transition in a girl with a mitochondrial disorder without a MELAS phenotype. Although the two base changes were adjacent to the 3243A > G mutation, they had different effects on the clinical phenotype, muscle pathology, and respiratory chain enzyme activity. Investigations of the different effects of the 3244G > A and 3242G > A base changes may provide a better understanding of tRNA dysfunction in mitochondrial disorders.

1. Introduction

Mutations in mitochondrial tRNA genes are the most common molecular causes of mitochondrial encephalomyopathies. In particular, many mutations have been reported in the mitochondrial $tRNA^{Leu(UUR)}$ gene, indicating that the region is a hot spot for mutations (MITOMAP: a Human Mitochondrial Genome Database, http://www.mitomap.org/). Among them, an A-to-G mutation at nucleotide position (np) 3243 was the first reported in the mitochondrial $tRNA^{Leu(UUR)}$ gene (Goto et al., 1990) and is the most prevalent mutation in all ethnicities. This mutation demonstrates defects at several levels. At the molecular level, it causes decreased protein synthesis (Chomyn et al., 1992), transcription termination impairment (Hess et al., 1991), and an anticodon modification abnormality (Yasukawa et al., 2000; Suzuki et al., 2002). At the cellular level, it is associated with heteroplasmy and typical mitochondrial morphological findings, such as ragged-red fibers and strong SDH-reactive blood vessels (Goto et al., 1990; Sakuta and Nonaka, 1989). At the organ level, the mutation is strongly associated with mitochondrial myopathy, encephalopathy, lactic acidosis, and stroke-like episodes (MELAS) (Goto et al., 1990, 1992).

Mutations in the mitochondrial $tRNA^{Leu(UUR)}$ gene demonstrate marked phenotypic variability, ranging from pure myopathy (Campos et al., 2001; Hadjigeorgiou et al., 1999) to MELAS; however, the pathogenicity of only a few mutations including 3243A > G has been confirmed. As new cases of tRNA mutations accumulate and are analyzed, we will develop an understanding of their pathogenesis and the genotype–phenotype relationship.

Here, we report two new cases harboring novel base changes at both sides of the 3243A > G mutation. One was a 3244G > A transition and the other was a 3242G > A transition. We studied these patients clinically, pathologically, biochemically, and genetically to determine the different effects of these novel base changes that are adjacent to the common 3243A > G mutation.

* Corresponding author. Tel.: +81 42 346 1713; fax: +81 42 346 1743.
E-mail address: goto@ncnp.go.jp (Y.-i. Goto).

1567-7249/$ - see front matter © 2009 Elsevier B.V. and Mitochondria Research Society. All rights reserved.
doi:10.1016/j.mito.2009.01.005

2. Materials and methods

2.1. Clinical investigations

2.1.1. Patient 1

Patient 1 was a 6-year-old girl born to nonconsanguinous parents after an uncomplicated pregnancy and birth. Her family history was unremarkable, including that of her mother and sister. At 4 years of age, she had an attack with vomiting followed by loss of consciousness, and clonic convulsions of the right arm. After the first attack, she had recurrent seizures with episodic vomiting and gradually developed psychomotor deterioration. She was unable to run by the age of 6. At that time, she could converse, but often counted incorrectly. Her limbs were atrophic, and her muscle tone and power were reduced. The patient had no cerebellar signs, myoclonus, or abnormalities of the cranial nerves. A laboratory examination revealed elevated lactate and pyruvate levels in the blood (lactate, 4.81 mmol/l; pyruvate, 0.117 mmol/l; normal, 0.44–1.33 and 0.045–0.113, respectively) and in the cerebrospinal fluid (lactate, 13.3 mmol/l; pyruvate, 0.451 mmol/l). Computed tomography (CT) of the brain revealed calcifications of the basal ganglia and diffuse cerebral atrophy (Fig. 1A). Magnetic resonance imaging (MRI) images of the brain showed diffuse abnormal high T2-weighted signals in the cerebral white matter, especially around the lateral ventricles, and multiple patchy T2-weighted signals in the cerebral cortex.

2.1.2. Patient 2

Patient 2 was a female born to nonconsanguinous parents. Her mother was healthy without any neurological symptoms. Her elder sister had a short stature due to Turner's syndrome with a typical 45X karyotype, but had no other symptoms of mitochondrial disorders. A birth weight of 1985 g at 37 weeks of gestation indicated intrauterine growth retardation. At birth, she had difficulty in sucking and became tachypneic and anemic, but she gradually improved and was discharged from the hospital. At 5 months of age, she was admitted to a hospital due to muscle floppiness and failure to thrive. She showed generalized hypotonia with absence of head control. She developed respiratory failure, heart failure, renal failure due to tubular dysfunction, and lactic acidosis, and therefore, she needed artificial ventilation. An echocardiogram indicated hypertrophic and dilatated cardiomyopathy. A laboratory examination revealed elevated lactate and pyruvate levels in the blood (lactate, 11.0 mmol/l; pyruvate, 0.31 mmol/l) and in the cerebrospinal fluid (lactate, 13.0 mmol/l; pyruvate, 0.44 mmol/l). She also had a significantly elevated creatine kinase (616 IU/l; normal, 43–170). CT and MRI images of the brain revealed nonspecific diffuse cerebral atrophy (Fig. 1A). After discharge from the hospital, she received artificial ventilation four times because of severe acidosis due to infection. However, after the age of 2 years, manifestations including acidosis, renal function, cardiac function, and muscle tonus slowly improved and she showed gradual psychomotor development without any deterioration.

Written informed consent was obtained from the parents of these patients to perform a muscle biopsy, molecular analysis, and biochemical studies.

2.2. Histopathological study

A biopsy from the *biceps brachii* muscle was frozen in isopentane chilled with liquid nitrogen, and serial frozen sections were stained with hematoxylin–eosin, modified Gomori trichrome (mGT), succinate dehydrogenase (SDH), cytochrome *c* oxidase (COX) by several histochemical methods.

2.3. Molecular genetic studies

DNA extraction, polymerase chain reaction (PCR), and total mitochondrial DNA (mtDNA) sequencing were performed, as described elsewhere (Akanuma et al., 2000). We applied the long

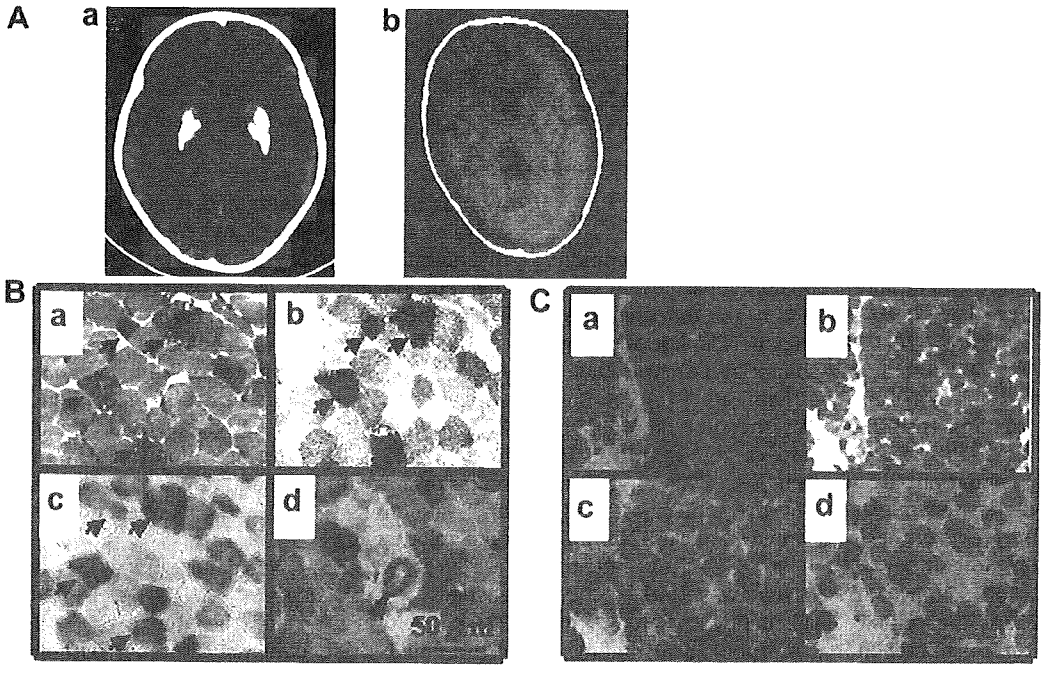

Fig. 1. Computed tomography and histochemical analysis. (A) Computed tomography of the brain of patient 1 (a) revealed calcifications of the basal ganglia and diffuse cerebral atrophy, and of patient 2 (b) revealed mild cerebral atrophy. Morphological analysis of the skeletal muscle of patient 1 (B) and patient 2 (C). In patient 1, ragged-red fibers (RRFs) (arrows) depicted by modified Gomori trichrome (a) and succinate dehydrogenase (SDH) stains. (b) Cytochrome *c* oxidase (COX) stain (c) revealed a focal COX deficiency, but most of the RRFs reflected intact COX activity (arrows). A strongly SDH-reactive blood vessel (SSV) was detected on the SDH stain (arrowhead). (d) In patient 2, hematoxylin–eosin (a) and modified Gomori trichrome (b) stain revealed moderate fiber size variation without RRFs, SDH, (c) and COX statin (d) showed subsarcolemmal accumulation of mitochondria (arrows) without COX-negative fibers.

PCR-based sequencing method to avoid any adverse results associated with similar sequences in the nuclear DNA. The sequence data were compared with the Human DNA Revised Cambridge Reference Sequence (MITOMAP: a Human Mitochondrial Genome Database; http://www.mitomap.org/mitomap/mitoseq.html).

We devised a real-time PCR amplification method based on a previously described approach (Komaki et al., 2003) to accurately quantify the frequency of the 3244G > A mutation. The target sequence (np 3211–3322) was amplified using a pair of primers and two fluorogenic TaqMan™ probes (PE Applied Biosystems; Foster City, CA, USA) designed for the wild-type and mutant sequences (Table 1). The copy number of mtDNA containing each mutant or wild-type sequence was determined based on a standard curve created by the reaction of a known amount of plasmid containing the mtDNA fragment (np 3171–3350) with each wild-type or mutant sequence.

To identify the 3242G > A transition, we amplified the 126-bp PCR fragment with the forward and mismatched primers and digested the fragment by SacI. If the fragment did not have the 3242G > A base change, then 108- and 18-bp cleaved fragments would be obtained. Each fragment was detected in a 4% agarose gel (Nusieve 3:1 agarose; Bio-Whittaker Molecular Applications; Rockland, ME, USA) stained with ethidium bromide.

2.4. Biochemical studies of primary cultures and transmitochondrial cell lines

Primary skin fibroblasts were obtained from patients 1 and 2, and myoblasts could be obtained only from patient 2. The fibroblasts and myoblasts were grown in DMEM/F-12 medium with 20% fetal bovine serum (Invitrogen Corp. Carlsbad, CA, USA).

Transmitochondrial cell lines (cybrids) were obtained by polyethylene glycol fusing of enucleated fibroblasts from both patients with human osteosarcoma 143B/TK- cells lacking mtDNA (King and Attardi, 1989). Twenty clones derived from patient 2 were selected from a uridine-lacking medium and employed to measure ATP synthesis and enzymatic activity of individual mitochondrial respiratory complexes. The DNA was extracted from each clone for the quantification of the proportions of the 3244G > A mutation. Cybrid cells derived from patient 2 were used to measure enzymatic activity of individual mitochondrial respiratory complexes and for blue native polyacrylamide gel electrophoresis (BN-PAGE).

The methods to measure ATP synthesis in digitonin-permeabilized fibroblasts, myoblasts, or cybrids is described elsewhere (Komaki et al., 2003), along with several modifications of a method reported by Robinson (Robinson, 1996).

Enzymatic activity of individual mitochondrial respiratory complexes was performed on isolated mitochondria obtained from cultured 5×10^5 cybrid and 143B/TK-cells according to Trounce et al. with modifications (Trounce et al., 1996). The activities of complexes I, IV, and citrate synthase were measured by spectrophotometric assays as described. All samples were measured at least in duplicate and averaged.

Table 1
Fluoroeenie probes mid amplification primers for real-time PCR.

Fluorogenic probes sequence		Primer sequence
Wild	5′ (FAM)-TGGCAGA GCCCGGT-(MGB) p3′	Forward 5′-CCACCCAAGAACAGGGTTTG-3′
Mutant	5′ (VIC)-TGGCAGAACCCGGT-(MGB) p3′	Reverse 5′-GGTTGGCCATGGGTATGTTG-3′

The underlined positions corresponded to np 3244. MGB: minor groove binder.

2.5. BN-PAGE and Western blot for immunodetection

Mitochondrial proteins were isolated from cultured 143B/TK-cells and cybrids derived from patient 2 ($3–6 \times 10^6$ cells) (Nijtmans et al., 2002). The mitochondrial proteins (100 μg) were solubilized in sample buffer (Invitrogen) containing 0.5% (w/v) *n*-dodecyl-β-d-maltoside (DDM). Electrophoresis was performed on 3–12% polyacrylamide gels (Invitrogen) (Nijtmans et al., 2002; D'Aurelio et al., 2006). Following BN-PAGE, the gels were soaked in a transfer buffer (Invitrogen) and blotted onto polyvinylidene fluoride (PVDF) membranes using the iBlot transfer system (Invitrogen) according to the manufacturer's instructions (20 V, 7 min). Subunit-specific mouse monoclonal antibodies (Molecular Probes) were used to immunodetect protein complexes. The cocktail of primary antibodies included the 39 kDa (complex I, 0.5 μg/mL), 70 kDa (complex II, 0.5 μg/mL), core II (complex III, 0.5 μg/mL), subunit I (complex IV, 2.5 μg/mL), and subunit β (complex V, 0.5 μg/mL). After removing the cocktail of primary antibodies, the alkaline phosphatase-conjugated anti-mouse secondary antibody was reacted, and nitroblue tetrazolium chloride (NBT)-derived chromogenic detection was performed. We determined the appropriate conditions to solubilize the mitochondrial membranes while preserving the intact respiratory chain complexes.

3. Results

3.1. Histopathological study

The histopathological study of the skeletal muscle from patient 1, at the age of 6 years, revealed the presence of numerous ragged-red fibers (RRFs), i.e., ⩾15% of the total fibers and some strongly succinate dehydrogenase-reactive blood vessels (SSVs). The COX stain revealed diffuse COX-negative fibers, whereas most of the RRFs were reactive (Fig. 1B). In patient 2, at the age of 9 months, there was increased subsarcolemmal accumulation of mitochondria in many fibers, which suggested mitochondrial abnormalities, but typical RRF, SSV, and COX-negative fibers were not detected (Fig. 1C).

3.2. Molecular genetic studies

No large-scale mtDNA rearrangements were detected by the long PCR method in either patient. Total mtDNA sequencing of the muscle from patient 1 revealed 38 base changes compared with the revised standard sequence (Table 2). According to the MITOMAP database, 37 changes have been previously reported as normal polymorphisms. One of the observed changes was a G-to-A mutation at np 3244 in the mitochondrial $tRNA^{Leu(UUR)}$ gene, and this change appeared to be heteroplasmic (i.e., both the mutant and the wild-type genome were present) on electropherograms (Fig. 2A). Real-time PCR amplification confirmed that the percentage of mutant mtDNA in the patient's muscle and fibroblasts was 94% and 90%, respectively. In patient 2, total mtDNA sequencing of muscle revealed 41 base changes compared with the standard sequence (Table 3). According to the MITOMAP database, 39 changes have been previously reported as normal polymorphisms. We identified a 6481T > C base change that had not been reported previously to the MITOMAP database; however, we detected this base change in her healthy mother. We also detected a G-to-A base change at np 3242 (Fig. 2B). This change was confirmed by restriction fragment polymorphism and was revealed to be homoplasmic (i.e., only the mutant genome was present) in the patient's tissues, including blood, but was absent in the blood of her healthy mother (Fig. 2C). Total mtDNA sequencing of blood from the proband's mother revealed the

Table 2
MtDNA sequence variants in patient 1.

Gene product	np	Base-change	Amino acid change	MitoMap database
D-loop	73	A to G		Reported polymorphism
D-loop	152	T to C		Reported polymorphism
D-loop	263	A to G		Reported polymorphism
D-loop	311	Insertion C		Reported polymorphism
D-loop	489	T to C		Reported polymorphism
12S rRNA	750	A to G		Reported polymorphism
16S rRNA	2706	A to G		Reported polymorphism
16S rRNA	3010	G to A		Reported polymorphism
16S rRNA	3206	C to T		Reported polymorphism
tRNA-Leu(UUR)	3244	G to A		Unreported
NADH dehydrogenase 2	4763	A to G	Synonymous	Reported polymorphism
NADH dehydrogenase 2	4883	C to T	Synonymous	Reported polymorphism
NADH dehydrogenase 2	5178	C to A	L to M	Reported polymorphism
Cytochrome c oxydase I	7028	C to T	Synonymous	Reported polymorphism
ATP synthase a	8414	C to T	L to F	Reported polymorphism
ATP synthase a	8473	T to C	Synonymous	Reported polymorphism
ATP synthase 0	8701	A to G	T to A	Reported polymorphism
ATP synthase 0	8860	A to G	T to A	Reported polymorphism
Cytochrome c oxydase 3	9540	T to C	Synonymous	Reported polymorphism
Cytochrome c oxydase 3	9524	T to C	Synonymous	Reported polymorphism
NADH dehydrogenase 3	10308	A to G	T to A	Reported polymorphism
NADH dehydrogenase 3	10400	C to T	Synonymous	Reported polymorphism
tRNA-Arg	10410	T to C		Reported polymorphism
NADH dehydrogenase 4	10873	T to C	Synonymous	Reported polymorphism
NADH dehydrogenase 4	11710	G to A	Synonymous	Reported polymorphism
NADH dehydrogenase 5	12706	C to T	Synonymous	Reported polymorphism
NADH dehydrogenase 6	14068	C to T	Synonymous	Reported polymorphism
Cytochrome b	14766	C to T	I to T	Reported polymorphism
Cytochrome b	14783	T to C	Synonymous	Reported polymorphism
Cytochrome b	14070	T to C	I to T	Reported polymorphism
Cytochrome b	15043	G to A	Synonymous	Reported polymorphism
Cytochrome b	15301	G to A	Synonymous	Reported polymorphism
Cytochrome b	15314	G to A	A to T	Reported polymorphism
Cytochrome b	15326	A to G	T to A	Reported polymorphism
D-loop	16085	C to T		Reported polymorphism
D-loop	16120	G to A		Reported polymorphism
D-loop	10223	C to T		Reported polymorphism
D-loop	10223	T to C		Reported polymorphism
D-loop	10500	T to C		Reported polymorphism

same polymorphisms except for the 3242G > A base change (data not shown).

3.3. Biochemical studies

In patient 1, fibroblast ATP synthesis was significantly low when pyruvate/malate or glutamate/malate were used as the substrate (Fig. 2D), but the rate of synthesis was normal when succinate or TMPD/ascorbate were added to the cells. These findings revealed that fibroblasts derived from this patient had a complex I deficiency. To confirm that the 3244 mutation was pathogenic, we performed functional analysis of cybrids. We obtained 20 clones with a different percentage of the heteroplasmic np 3244 mutation and performed ATP synthesis assays using each clone. ATP synthesis was within the normal range when the percentage of mutant DNA remained under 90%. Clones carrying mutant mtDNA in high proportions, i.e., those exceeding the threshold level of approximately 95%, lost their ability to synthesize ATP when glutamate/malate or TMPD/ascorbate were used as the substrate (Fig. 2E,F). Moreover, analysis of enzymatic activity for individual mitochondrial respiratory complexes revealed that the activities of complexes I and II were apparently low in the cybrid cells carrying a high proportion of mutant mtDNA, although they were normal in cybrid cells carrying a low proportion of mutant mtDNA (Fig. 2G). These findings indicated that extremely high levels of the mutation led not only to a complex I deficiency, but also to complex IV and/or V deficiencies.

In contrast, the fibroblasts and myoblasts of patient 2 showed normal ATP synthesis (data not shown); however, her cybrid cells had low levels of complex IV activity (Fig. 2G).

3.4. Studies on assembly of respiratory chain enzymes

To understand the consequences of the 3242G > A mutation on the composition of the respiratory chain, BN-PAGE analysis was performed using the subunit-specific monoclonal antibodies on equal amounts of mitochondrial proteins extracted from the same number of mutant cybrids and human osteosarcoma 143B/TK- cells. Also, the amount of assembled respiratory chain complexes in cybrid clones carrying the 3242G > A mutation was estimated. Compared with 143B/TK-, cybrids showed a reduced level of the complex I-III-IV supercomplex and an increase in the amount of the complex I-III supercomplex. The levels of the complex III homodimer and complex II were assessed as a loading control (Fig. 2H).

4. Discussion

MELAS is a maternally inherited disorder typically characterized by onset before the age 15 years, lactic acidosis, episodic vomiting, seizures, migraine-like headaches, and recurrent cerebral insults resembling strokes (Goto, 1995; Hirano and Pravlakis, 1994). The symptoms of patient 1, including the onset age, recurrent episodic vomiting, headache, hemiconvulsions, and severe lactic acidosis, were consistent with the clinical spectrum associated

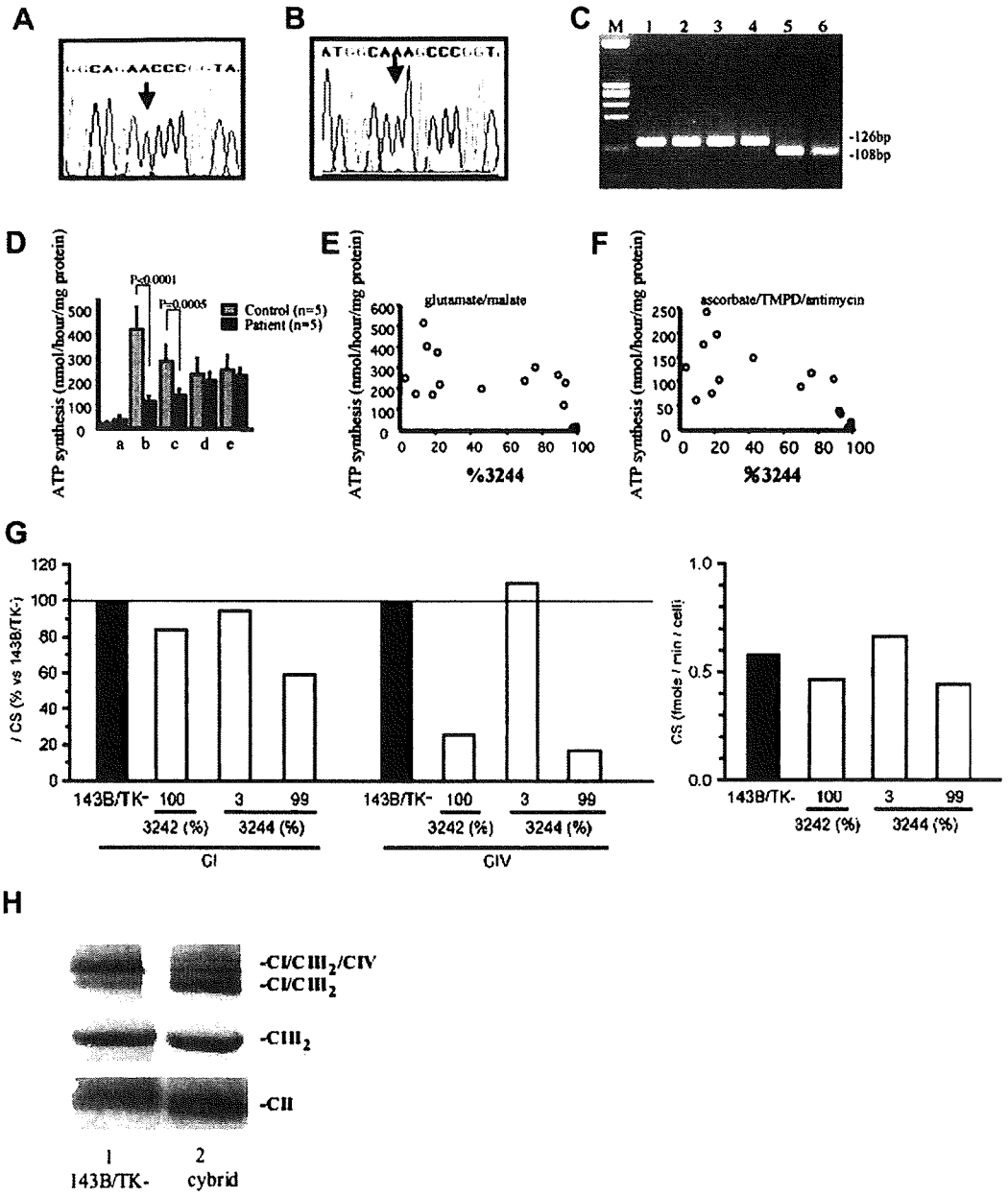

Fig. 2. Molecular and biochemical analysis. (A) An electropherogram based on mtDNA sequencing from muscle specimens revealed a heteroplasmic G-to-A substitution at nucleotide position 3244 (arrow) in the $tRNA^{Leu(UUR)}$ gene of patient 1, and a (B) G-to-A substitution at nucleotide position 3242 (arrow) in patient 2. (C) SacI digestion of the mutant 3242G > A mtDNA is indicated by a 126-bp band. Wild-type mtDNA is indicated by the presence of a 108-bp band. M, molecular weight markers; lane 1, patient's muscle; lane 2, myoblast; lane 3, fibroblast; lane 4, blood; lane 5, mother's blood; lane 6, wild-type control. (D) ATP synthesis in a digitonin-treated primary culture of fibroblasts with 90% mutants. ATP synthesis was measured using the following combinations of substrates and specific inhibitors: a, none; b, pyruvate/malate; c, glutamate/malate; d, succinate/rotenone; e, ascorbate/TMPD/antimycin. The results of this assay are expressed as nanomoles ATP per hour per milligram of cell protein. The control values are presented as the mean ±1 SD. ATP synthesis in 143B/TK- derived cybrid clones with various percentages of the 3244G > A mutation (open circles) and 143B/TK- cells (closed circles). (E) Glutamate + malate was used as the substrate. (F) Ascorbate and TMPD were used as the substrates, and antimycin was used as an inhibitor. (G) Activities of the respiratory chain complexes relative to citrate synthase in 143B/TK- cells and cybrid clones carrying the 3242G > A mutation (100% mutant) and the 3244G > A mutation (3% and 99% mutant). The figure to the right shows the activity of citrate synthase in these clones. CI, complex I; CIV, complex IV; CS, citrate synthase. (H) $CI/CIII_2/CIV$ supercomplex level decreases and $CI/CIII_2$ supercomplex level increases in cybrid clones carrying the 3242G > A mutation (lane 2), compared to 143B/TK-cells (lane 1). $CI/CIII_2/CIV$, complex I-III-IV supercomplex; $CI/CIII_2$, complex I-III supercomplex; $CIII_2$, complex III homodimer; CII, monomeric complex II.

with MELAS. Morphological analysis of the muscle biopsy also showed typical findings of MELAS. We detected diffuse COX-negative fibers and numerous RRFs, some of which stained positive for COX activity, as has previously been reported in MELAS patients but not in those with other mitochondrial myopathies (Goto et al., 1992). We also observed SSVs, which is an important finding in MELAS patients (Hasegawa et al., 1991). Patient 2 showed multiple tissue involvement including severe lactic acidosis, cardiomyopathy, renal tubular dysfunction, cerebral atrophy, generalized hypotonia in infancy, and increased subsarcolemmal accumulation of mitochondria in the muscle biopsy, which strongly suggested that she had a mitochondrial disease. However, the clinical picture and pathological findings were apparently different from MELAS.

The underlying molecular defects involved in these cases were distinct from the common causes of mitochondrial disorders including MELAS. Here, none of the previously reported pathogenic

Table 3
MtDNA sequence variants m patient 2.

Gene product	np	Base change	Amino acid change	MitoMap database
D-loop	73	A to G		Reported polymorphism
D-loop	152	T to C		Reported polymorphism
D-loop	263	A to G		Reported polymorphism
D-loop	303	Insertion C		Reported polymorphism
D-loop	311	Insertion C		Reported polymorphism
D-loop	480	T to C		Reported polymorphism
12S rRNA	750	A to G		Reported polymorphism
12S rRNA	1438	A to G		Reported polymorphism
16S rRNA	2706	A to G		Reported polymorphism
16S rRNA	3010	G to A		Reported polymorphism
16S rRNA	3206	C to T		Reported polymorphism
tRNA-Leu(UUR)	3242	G to A		Unreported
NADH dehydrogenase 2	4760	A to G	Synonymous	Reported polymorphism
NADH dehydrogenase 2	4883	C to T	Synonymous	Reported polymorphism
NADH dehydrogenase 2	5173	C to A	L to M	Reported polymorphism
NADH dehydrogenase 2	5201	G to A	A to T	Reported polymorphism
Cytochrome c oxydase I	6481	T to C	V to A	Unreported
Cytochrome c oxydase I	7028	C to T	Synonymous	Reported polymorphism
ATP synthase 8	8414	C to T	L to F	Reported polymorphism
ATP synthase 8	8473	T to C	Synonymous	Reported polymorphism
ATP synthase 6	3701	A to G	T to A	Reported polymorphism
ATP synthase 6	8860	A to G	T to A	Reported polymorphism
Cytochrome c oxydase 3	8540	T to C	Synonymous	Reported polymorphism
NADH dehydrogenase 3	10,308	A to G	T to A	Reported polymorphism
NADH dehydrogenase 3	10,400	C to T	Synonymous	Reported polymorphism
tRNA-Arg	10,410	T to C		Reported polymorphism
NADH dehydrogenase 4	10,873	T to C	Synonymous	Reported polymorphism
NADH dehydrogenase 4	11,710	G to A	Synonymous	Reported polymorphism
NADH dehydrogenase 5	12,706	C to T	Synonymous	Reported polymorphism
NADH dehydrogenase 6	14,068	C to T	Synonymous	Reported polymorphism
Cytochrome b	14,766	C to T	I to T	Reported polymorphism
Cytochrome b	14,783	T to C	Synonymous	Reported polymorphism
Cytochrome b	14,870	T to C	I to T	Reported polymorphism
Cytochrome b	15,043	G to A	Synonymous	Reported polymorphism
Cytochrome b	15,301	G to A	Synonymous	Reported polymorphism
Cytochrome b	15,314	G to A	A to T	Reported polymorphism
Cytochrome b	15,320	A to G	T to A	Reported polymorphism
D-loop	16,120	G to A		Reported polymorphism
D-loop	16,223	C to T		Reported polymorphism

The T64S1C base change was observed in a healthy mother of patient 2.

mutations of mtDNA were found, but we did identify base changes adjacent to the 3243A > G mutation, which is the most common mutation in MELAS patients, including a 3244G > A transition in patient 1 and a 3242G > A transition in patient 2 (Fig. 3A). The 3244G > A and 3242G > A base changes have not been reported clinically, but as a somatic mutation in gastric carcinoma (Habano et al., 2000) and in the bone marrow of a patient with myelodysplastic syndrome (Gattermann et al., 2004), respectively.

Several lines of evidence support a causal association between the 3244G > A base change mutation and MELAS. First, this base change was not observed in over 200 normal individuals. Second, the 3244G > A transition disrupted a highly conserved nucleotide in the tRNA structure (Fig. 3B). Third, most mutations in typical cases of MELAS were located in the same tRNA gene, including the 3271T > C (Goto et al., 1991), 3291T > C (Goto et al., 1994), 3252A > G (Morten et al., 1993), and 3260A > G mutations (Nishino et al., 1996). Moreover, the 3244G > A base change was located adjacent to the most common mutation in MELAS patients, namely, the 3243A > G mutation (Fig. 3A). Fourth, this mutation existed under heteroplasmic conditions, which is a common feature of pathogenic mtDNA mutations. Finally, a functional analysis of cybrids revealed a significant decrease in the respiratory chain function, which was observed in cells with a relatively high percentage of mutant mtDNA. The results of these assays indicated deficiencies of complexes I and IV and a threshold effect of mutant load on respiratory chain enzyme activity, which has often been observed in MELAS patients carrying the 3243A > G mutation (Goto, 1995; Koga et al., 1995).

In patient 2, 6481T > C and 3242G > A base changes were detected; these polymorphisms were not reported previously. The 6481T > C change resulted in the replacement of valine with alanine; however, we detected this base change in her healthy mother. Therefore, it is reasonable to conclude that this base change is not pathogenic. In patient 2, the 3242G > A base change existed in all tissues in a homoplasmic condition, which is different than the 3244G > A or the more common 3243A > G mutation (Fig. 2C), thus making its pathogenicity difficult to confirm. However, there is evidence, including the biochemical defects in cybrid cells, to support the pathogenicity of this base change (Chinnery et al., 1999; McFarland et al., 2004). First, this transition was segregated with the disease; it was not detected in more than 200 normal individuals. Moreover, it was not detected in the blood of her healthy mother, although the base change was present in blood of the proband (Fig. 2C). Second, the 3242G > A transition affected a highly conserved position in the $tRNA^{Leu(UUR)}$ gene (Fig. 3B). Third, pathogenic mutations of several mitochondrial diseases have involved the dihydrouridine (DHU) stem of this tRNA (Kawarai et al., 1997; Nishigaki et al., 2003; Hao and Moraes, 1996). It is important to note that the DHU stem appears to be a rather weak structure and might thus be more prone to alterations leading to structural disturbances. The 3242G > A transition can alter the secondary and possibly the tertiary structure of the DHU-stem due to

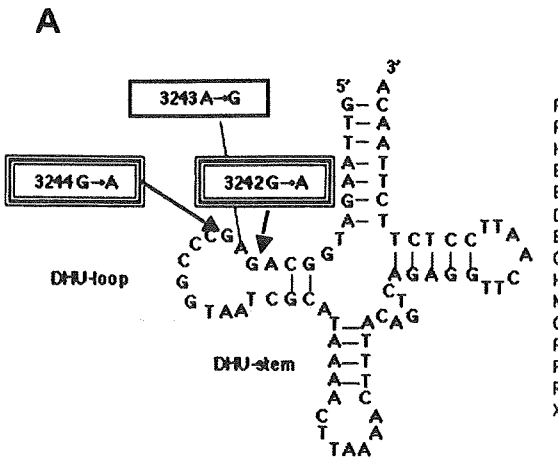

Fig. 3. (A) Secondary structure of the human mitochondrial $tRNA^{Leu(UUR)}$ gene and positions of the 3242G > A, 3243A > G, and 3244G > A mutations. (B) Comparison of mitochondrial $tRNA^{Leu(UUR)}$ among several species. 3242G > A and 3244G > A mutations are boxed.

"strengthening" of the stem by the formation of an additional A–U pairing instead of the well-conserved C–U pair (Helm et al., 2000) (Fig. 3A). Fourth, a somatic mutation of the 3242G > A was recently detected in CD34+ bone marrow cells, but not in peripheral blood cells (Gattermann et al., 2004). The authors supported the pathogenicity of this mutation, which they thought was associated with a maturation defect, and that the dysfunction of the mitochondria carrying the mutation contributed to ineffective hematopoiesis in their patient. Finally, we found that the cybrid cells carrying the 3242G > A mutation derived from patient 2, which excluded any influence of nuclear genes, revealed the functional defect of the mutation; the enzymatic activity of complex IV was apparently low in cybrid cells and the BN-PAGE analysis of the cybrid cells showed a reduced level of the complex I–III–IV supercomplex and an increase in the complex I–III supercomplex. Recently, an abnormal respiratory supercomplex was reported in a human disease (McKenzie et al., 2006). They proposed that unstable respiratory chain supercomplexes affect respiratory activities and subsequent pathology. In our case, the above findings suggest that the destabilization of the supercomplex due to the dissociation of complex IV is related to the activity of complex IV.

Point mutations at many of the 75 nucleotides in the $tRNA^{Leu(UUR)}$ gene have been associated with several distinct mitochondrial diseases with variable phenotypes ranging from pure myopathy to multisystemic disorders such as MELAS (Campos et al., 2001; Hadjigeorgiou et al., 1999; Goto et al., 1990; Sevidei, 2002; Moraes et al., 1992; Seneca et al., 2001; Jaksch et al., 2001). However, the reasons for the differences between the genotypes and phenotypes are not clear. The novel 3244G > A mutation emphasizes the crucial role of $tRNA^{Leu(UUR)}$ dysfunction in the pathogenesis of MELAS. Because its biochemical effects were similar to those of the 3243A > G mutation, this portion of the tRNA gene is likely to be very important for the maintenance of tRNA function. However, the effects of the 3242G > A base change in the DHU stem on the clinical phenotype, pathological findings, and biochemical functions are different from those of the 3243A > G mutation. Because both novel base changes are adjacent to the common 3243A > G mutation, these different effects may be a key to clarify the molecular pathogenesis of mitochondrial disorders including MELAS.

Regarding the pathogenesis of the $tRNA^{Leu(UUR)}$ gene mutations including the 3243A > G mutation, several groups have pointed out the possibility of an abnormality at the transcription level, because these mutations occur in a control region responsible for the termination of transcription at the end of rRNA genes (Hess et al., 1991; King et al., 1992). Other groups have demonstrated that this type of mutant tRNA may be functionally deficient (Yasukawa et al., 2000; Chomyn et al., 2000). One of the groups revealed a specific correlation between the modification deficiency in mutant tRNA and the clinical features of mitochondrial disorders (Kirino et al., 2005). They reported that mitochondrial $tRNA^{Leu(UUR)}$ harboring mutations, such as the 3244G > A transition, detected in tissues from patients with symptoms of MELAS lacked the normal taurine-containing modification at the anticodon wobble position. In contrast, mitochondrial $tRNA^{Leu(UUR)}$ with mutations, including the 3242G > A transition, detected in patients that have mitochondrial diseases but do not show the MELAS symptoms had the normal modifications. Further investigations of the different effects of the np 3244 and np 3242 base changes on the phenotypes and the similarities shared by the np 3243 and 3244 base changes may provide clues for elucidating the actual impact of $tRNA^{Leu(UUR)}$ gene mutations on the phenotypic expression of MELAS. The present results can contribute to a better understanding of tRNA function and provide insight into the complicated issues surrounding the association between genotype and phenotype in mitochondrial disorders.

Acknowledgements

We thank Mayuko Kato, Mitsuko Tanabe, and Munemitsu Yuasa for technical assistance. This work was supported in part by a Research Grant (15B-4, 18A-5) for Nervous and Mental Disorders from the Ministry of Health, Labor and Welfare of Japan (Y.G.), and a grant of the Comprehensive Research Project on Health Sciences Focusing on Drug Innovation (KHD2207) from the Japan Health Sciences Foundation (Y.G.).

References

Akanuma, J., Muraki, K., Komaki, H., Nonaka, I., Goto, Y., 2000. Two pathogenic point mutations exist in the authentic mitochondrial genome, not in the nuclear pseudogene. J. Hum. Genet. 45, 337–341.

Campos, Y., Gamez, J., Garcia, A., Andreu, A.L., Rubio, J.C., Martin, M.A., del Hoyo, P., Navarro, C., Cervera, C., Garesse, R., Arenas, J., 2001. A new mtDNA mutation in the $tRNA^{Leu(UUR)}$ gene associated with ocular myopathy. Neuromuscul. Disord. 1, 477–480.

Chinnery, P.F., Howell, N., Andrews, R.M., Turnbull, D.M., 1999. Mitochondria DNA analysis: polymorphisms and pathogenicity. J. Med. Genet. 36, 505–510.

Chomyn, A., Martinuzzi, A., Yoneda, M., Daga, A., Hurko, O., Johns, D., Lai, S.T., Nonaka, I., Angelini, C., Attardi, G., 1992. MELAS mutation in mtDNA binding site for transcription termination factor causes defects in protein synthesis and in respiration but no change in levels of upstream and downstream mature transcripts. Proc. Natl. Acad. Sci. USA 89, 4221–4225.

Chomyn, A., Enriquez, J.A., Micol, V., Fernandez-Silva, P., Attardi, G., 2000. The mitochondrial myopathy, encephalopathy, lactic acidosis, and stroke-like

episode syndrome-associated human mitochondrial tRNA$^{Leu(UUR)}$ mutation causes aminoacylation deficiency and concomitant reduced association of mRNA with ribosomes. J. Biol. Chem. 275, 19198–19209.
D'Aurelio, M., Gajewski, C.D., Lenaz, G., Manfredi, G., 2006. Respiratory chain supercomplexes set the threshold for respiration defects in human mtDNA mutant cybrids. Hum. Mol. Genet. 15, 2157–2169.
Gattermann, N., Wulfert, M., Junge, B., Germing, U., Haas, R., Hofhaus, G., 2004. Ineffective hematopoiesis linked with a mitochondrial tRNA mutation (3242G > A) in a patient with myelodysplastic syndrome. Blood 103, 1499–1502.
Goto, Y., 1995. Clinical features of MELAS and mitochondrial DNA mutations. Muscle Nerve 3, S107–112.
Goto, Y., Nonaka, I., Horai, S., 1990. A mutation in the tRNA$^{Leu(UUR)}$ gene associated with the MELAS subgroup of mitochondrial encephalopathies. Nature 348, 651–653.
Goto, Y., Nonaka, I., Horai, S., 1991. A new mtDNA mutation associated with mitochondrial myopathy, encephalopathy, lactic acidosis, and stroke-like episodes (MELAS). Biochim. Biophys. Acta 1097, 238–240.
Goto, Y., Horai, S., Matsuoka, T., Koga, Y., Nihei, K., Kobayashi, M., Nonaka, I., 1992. Mitochondrial myopathy, encephalopathy, lactic acidosis, and stroke-like episodes (MELAS): a correlative study of the clinical features and mitochondrial DNA mutation. Neurology 42, 545–550.
Goto, Y., Tsugane, K., Tanabe, Y., Nonaka, I., Horai, S., 1994. A new point mutation at nucleotide pair 3291 of the mitochondrial tRNA$^{Leu(UUR)}$ gene in a patient with mitochondrial myopathy, encephalopathy, lactic acidosis, and stroke-like episodes (MELAS). Biochem. Biophys. Res. Commun. 202, 1624–1630.
Habano, W., Sugai, T., Nakamura, S.I., Uesugi, N., Yoshida, T., Sasou, S., 2000. Microsatellite instability and mutation of mitochondrial and nuclear DNA in gastric carcinoma. Gastroenterology 118, 835–841.
Hadjigeorgiou, G.M., Kim, S.H., Fischbeck, K.H., Andreu, A.L., Berry, G.T., Bingham, P., Shanske, S., Bonilla, E., DiMauro, S., 1999. A new mitochondrial DNA mutation (A3288G) in the tRNA$^{Leu(UUR)}$ gene associated with familial myopathy. J. Neurol. Sci. 164, 153–157.
Hao, H., Moraes, C.T., 1996. Functional and molecular mitochondrial abnormalities associated with C->T transition at position 3256 of the human mitochondrial genome. J. Biol. Chem. 271, 2347–2352.
Hasegawa, H., Matsuoka, T., Goto, Y., Nonaka, I., 1991. Strongly succinate dehydrogenase-reactive blood vessels in muscles from patients with mitochondrial myopathy, encephalopathy lactic acidosis, and stroke-like episodes. Ann. Neurol. 29, 601–605.
Helm, M., Brule, H., Friede, D., Giege, R., Putz, D., Florentz, C., 2000. Search for characteristic structural features or mammalian mitochondrial tRNAs. RNA 6, 1356–1379.
Hess, J.F., Parisi, M.A., Bennett, J.L., Clayton, D.A., 1991. Impairment of mitochondrial transcription termination by a point mutation associated with the MELAS subgroup of mitochondrial encephalomyopathies. Nature 351, 236–239.
Hirano, M., Pravlakis, S., 1994. Mitochondrial myopathy, encephalopathy, lactic acidosis, and stroke-like episodes (MELAS): current concepts. J. Child Neurol. 9, 4–13.
Jaksch, M., Lochmuller, H., Schmitt, F., Volpel, B., Obermaier-Kusser, B., Horvath, R., 2001. A mutation in mt tRNA$^{Leu(UUR)}$ causing a neuropsychiatric syndrome with depression and cataract. Neurology 57, 1930–1931.
Kawarai, T., Kawakami, H., Kozuka, K., Izumi, Y., Matsuyama, Z., Watanabe, C., Kohriyama, T., Nakamura, S., 1997. A new mitochondrial DNA mutation associated with mitochondrial myopathy: tRNA$^{Leu(UUR)}$ 3254C-to-G. Neurology 49, 598–600.
King, M.P., Attardi, G., 1989. Human cells lacking mtDNA: repopulation with exogenous mitochondria by complementation. Science 246, 500–503.
King, M.P., Koga, Y., Davidson, M., Schon, E.A., 1992. Defects in mitochondrial protein synthesis and respiratory chain activity segregate with the tRNA$^{Leu(UUR)}$ mutation associated with mitochondrial myopathy, encephalopathy, lactic acidosis, and stroke-like episodes. Mol. Cell Biol. 12, 480–490.
Kirino, Y., Goto, Y., Campos, Y., Arenas, J., Suzuki, T., 2005. Specific correlation between the wobble modification deficiency in mutant tRNAs and the clinical features of a human mitochondrial disease. Proc. Natl. Acad. Sci. USA 102, 7127–7132.
Koga, Y., Davidson, M., Schon, E.A., King, M.P., 1995. Analysis of cybrids harboring MELAS mutations in the mitochondrial tRNAs$^{Leu(UUR)}$ gene. Muscle Nerve 3, S119–123.
Komaki, H., Akauma, J., Iwata, H., Takahashi, T., Mashima, Y., Nonaka, I., Goto, Y., 2003. A novel mtDNA C11777A mutation in Leigh syndrome. Mitochondrion 2, 293–304.
McFarland, R., Elson, J.L., Taylor, R.W., Howell, N., Turnbull, D.M., 2004. Assigning pathogenicity to mitochondrial tRNA mutations: when 'definitely maybe' is not good enough. Trends Genet. 20, 591–596.
McKenzie, M., Lazarou, M., Thorborn, D.R., Ryan, M.T., 2006. Mitochondrial respiratory chain supercomplexes are destabilized in Barth syndrome patients. J. Mol. Biol. 361, 462–469.
Moraes, C.T., Ricci, E., Bonilla, E., DiMauro, S., Schon, E.A., 1992. The mitochondrial tRNA$^{Leu(UUR)}$ mutation in mitochondrial encephalomyopathy, lactic acidosis, and stroke-like episodes (MELAS): genetic, biochemical, and morphological correlation in skeletal muscle. Am. J. Hum. Genet. 50, 934–949.
Morten, K.J., Cooper, J.M., Brown, G.K., Lake, B.D., Pike, D., Poulton, J., 1993. A new point mutation associated with mitochondrial encephalomyopathy. Hum. Mol. Genet. 2, 2081–2087.
Nijtmans, L.G., Henderson, N.S., Holt, I.J., 2002. Blue native electrophoresis to study mitochondrial and other protein complexes. Methods 26, 327–334.
Nishigaki, Y., Tadesse, S., Bonilla, E., Shungu, D., Hersh, S., Keats, B.J., Berlin, C.I., Goldverg, M.F., Vockley, J., DiMauro, S., Hirano, M., 2003. A novel mitochondrial tRNA$^{Leu(UUR)}$ mutation in a patient with features of MERRF and Kearns-Sayre syndrome. Neuromuscul. Disord. 13, 334–340.
Nishino, I., Komatsu, M., Kodama, S., Horai, S., Nonaka, I., Goto, Y., 1996. The 3260 mutation in mitochondrial DNA can cause mitochondrial myopathy, encephalopathy, lactic acidosis, and stroke-like episodes (MELAS). Muscle Nerve 19, 1603–1604.
Robinson, B.H., 1996. Use of fibroblast and lymphoblast cultures for detection of respiratory chain defects. In: Attardi, G.M., Chomyin, A. (Eds.), Methods in Enzymology, No. 264. Academic Press USA, San Diego, CA, pp. 454–463.
Sakuta, R., Nonaka, I., 1989. Vascular involvement in mitochondrial myopathy. Ann. Neurol. 25, 594–601.
Seneca, S., Verhelst, H., De Meirleir, L., Meire, F., Ceuterick-De Goote, C., Lissens, W., Van Coster, R., 2001. A new mitochondrial point mutation in the transfer RNA$^{Leu(UUR)}$ gene in a patient with a clinical phenotype resembling Kearn-Sayre syndrome. Arch. Neurol. 58, 1113–1118.
Sevidei, S., 2002. Mitochondrial encephalomyopathies: gene mutation. Neuromuscul. Disord. 12, 524–529.
Suzuki, T., Suzuki, T., Wada, T., Saigo, K., Watanabe, K., 2002. Taurine as a constituent of mitochondrial tRNAs: new insights into the functions of taurine and human mitochondrial diseases. EMBO J. 21, 6581–6589.
Trounce, I.A., Kim, Y.L., Jun, A.S., Wallace, D.C., 1996. Assessment of mitochondrial oxidative phosphorylation in patient muscle biopsies, lymphoblasts, and transmitochondrial cell lines. In: Attardi, G.M., Chomyin, A. (Eds.), Methods in Enzymology, No. 264. Academic Press USA, San Diego, CA, pp. 484–509.
Yasukawa, T., Suzuki, T., Ueda, T., Ohta, S., Watanabe, K., 2000. Modification defect at anticodon wobble nucleotide of mitochondrial tRNAs$^{Leu(UUR)}$ with pathogenic mutations of mitochondrial myopathy, encephalopathy, lactic acidosis, and stroke-like episodes. J. Biol. Chem. 275, 4251–4257.

Journal of the Neurological Sciences 278 (2009) 35–40

Contents lists available at ScienceDirect

Journal of the Neurological Sciences

journal homepage: www.elsevier.com/locate/jns

Progressive carotid artery stenosis with a novel tRNA phenylalanine mitochondrial DNA mutation

Takahiro Iizuka [a,*], Yu-ichi Goto [b], Saori Miyakawa [a], Mayumi Sato [a], Zhaoxia Wang [b], Kosuke Suzuki [a], Junichi Hamada [a], Akira Kurata [c], Fumihiko Sakai [a]

[a] Department of Neurology, School of Medicine, Kitasato University, Kanagawa, Japan
[b] Department of Mental Retardation and Birth Defect Research, National Institute of Neuroscience, National Center of Neurology and Psychiatry, Japan
[c] Department of Neurosurgery, School of Medicine, Kitasato University, Kanagawa, Japan

ARTICLE INFO

Article history:
Received 7 August 2008
Received in revised form 7 November 2008
Accepted 12 November 2008
Available online 16 December 2008

Keywords:
Carotid stenosis
Brain infarction
Mitochondrial encephalopathy
Carotid stenting
Gene mutation

ABSTRACT

Mitochondrial myopathy, encephalopathy, lactic acidosis and stroke-like episodes (MELAS) is a distinct clinical syndrome caused by mutations in the mitochondrial DNA. The pathogenesis of stroke-like episodes remains unknown but major vessels stenosis is not a cause of stroke-like episodes. We describe a novel heteroplasmic G617A transition in the mitochondrial transfer RNA phenylalanine gene in a patient with encephalomyopathy who presented with recurrent embolic ischemic strokes accompanied by transient occlusion of middle cerebral, anterior cerebral and internal carotid arteries. These ischemic strokes were presumed to be artery-to artery embolisms associated with carotid artery stenosis. Single muscle fiber analysis revealed the pathogenicity of the mutation although its causative role on carotid artery stenosis remains to be elucidated. This case expands phenotypic spectrum of mitochondrial disorders in terms of macroangiopathy, but macroangiopathy-related ischemic strokes should be distinguished from *classic stroke-like episodes* of MELAS that are speculated to be microangioapthy-related or non-ischemic neurovascular events.

1. Introduction

Mitochondrial myopathy, encephalopathy, lactic acidosis and stroke-like episodes (MELAS) is a distinct clinical syndrome of respiratory-chain disorder caused by mutations in the mitochondrial DNA (mtDNA) [1]. Most of the mutations are located in the mitochondrial transfer RNA (tRNA)$^{LEU(UUR)}$ gene, but mutations in other tRNA genes or polypeptide-coding genes have been identified in MELAS or MELAS overlapping syndrome. Phenotypic–genotypic variation is emphasized accordingly, but the original definition of MELAS becomes blurred [2]. "Stroke-like episode" is a distinct feature of MELAS but it has never been clearly defined yet [3]. Thus, "stroke-like episode" or "ischemic stroke" may have been used ambiguously without clear distinction in mitochondrial disorders [4,5]. We previously reported that stroke-like episodes of MELAS are non-ischemic neurovascular cellular events presumably associated with neuronal hyperexcitability, which is a different pathophysiology from ischemic stroke [2,6,7].

We now report on a case of mitochondrial encephalomyopathy with a novel mtDNA mutation, who presented with ischemic stroke accompanied by recurrent occlusion of major cervicocerebral arteries.

2. Case report

This 40-year-old left-handed Japanese man began to have brain infarction since the age of 35 years. He was the second son of unrelated parents. His mother and elder brother had no significant medical history including diabetes, hearing loss, headache or other symptoms associated with mitochondrial disorders. His farther had a history of ischemic heart disease. His psychomotor development appeared normal until 8 years when mental retardation and hearing impairment were noticed. He developed diabetic ketoacidosis at age 30, since then he began to receive insulin. He underwent cataract surgery at age 33. At age 35, he was admitted to this hospital four days after onset of left hand clumsiness and transient dysarthria.

On admission, physical examination was unremarkable except short stature (148 cm). He had minimal left hand weakness and bilateral sensorineural hearing loss of 60 dB. He achieved a performance IQ of 53, verbal IQ 56 and full-scale IQ 49. Diffusion-weighted MRI (DWI) showed acute cortical infarction in the right middle cerebral artery (MCA) territories (Fig. 1A), but intracranial three-dimensional (3D) time-of flight (TOF) MR angiography (MRA) was normal (Fig. 1B). Cervical MRA was not performed. Blood/CSF tests were normal except HbA1c 8.0%, serum lactate 2.13 mmol/L (normal; 0.44–1.89), and CSF lactate 4.57 mmol/L (normal; 1.40–1.48). A diagnosis of MELAS was suspected, but no A3243G or T3271C mutation was detected in blood. He was discharged without antiplatelet agent.

* Corresponding author. Department of Neurology, School of Medicine, Kitasato University, 1-15-1 Kitasato, Sagamihara, Kanagawa, 228-8555, Japan. Tel.: +81 42 778 8136; fax: +81 42 778 6400.
E-mail address: takahiro@med.kitasato-u.ac.jp (T. Iizuka).

0022-510X/$ – see front matter © 2008 Elsevier B.V. All rights reserved.
doi:10.1016/j.jns.2008.11.016

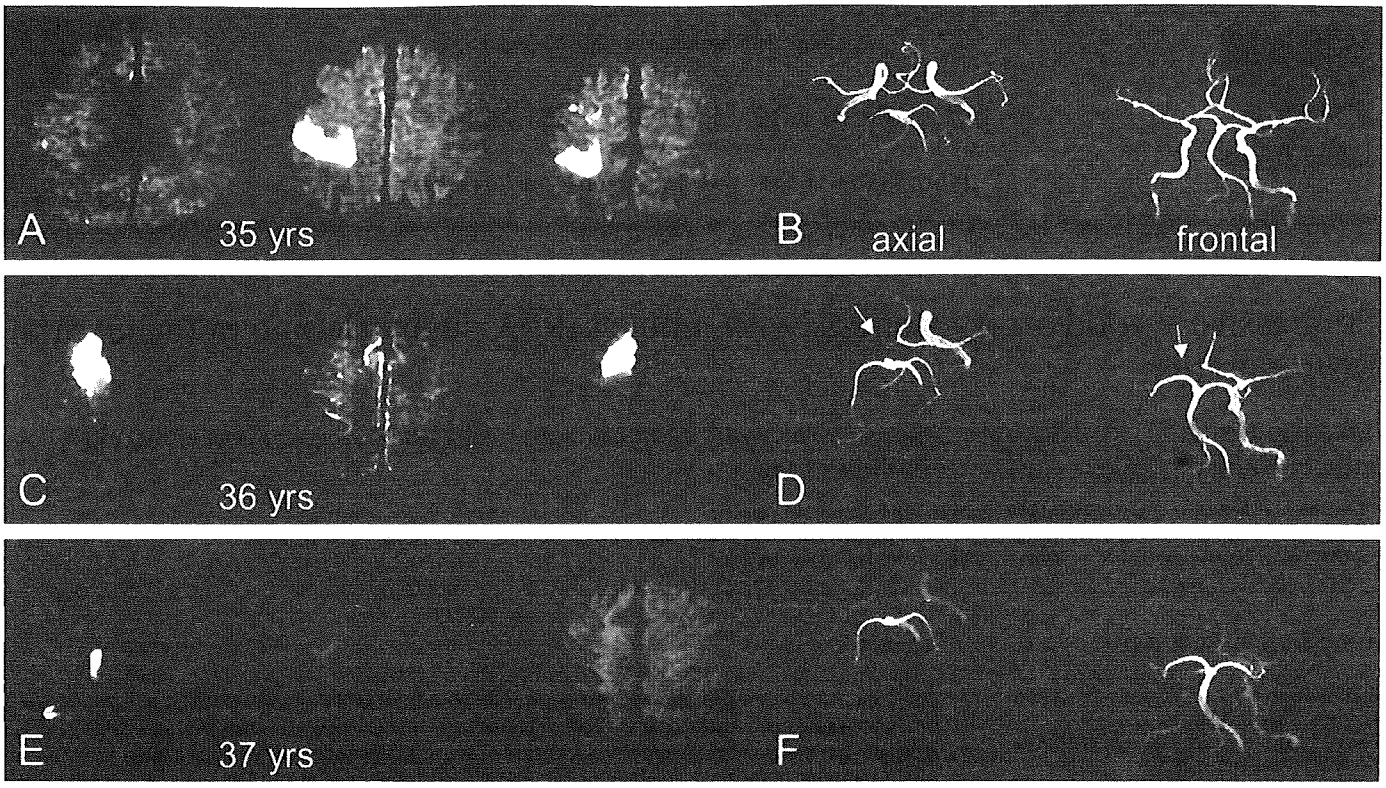

Fig. 1. Serial diffusion-weighted MRI and MR angiography during each stroke event. DWI on admission of the first stroke at age 35 years shows acute ischemic lesions in the right MCA territories (A), but intracranial 3D-TOF MRA was normal (B). DWI on admission of the second stroke at age 36 years showed acute ischemic lesions in the right both MCA and ACA territories (C). MRA shows loss of signal of the right ICA and MCA, but distal A1 segment remains visible (D, arrow). DWI obtained on day 3 of onset of the third stroke shows scattered ischemic lesions in the cortico-subcortical regions in the right MCA territories (E). MRA reveals loss of the right MCA (F). These ischemic lesions are different from those of stroke-like episodes of MELAS.

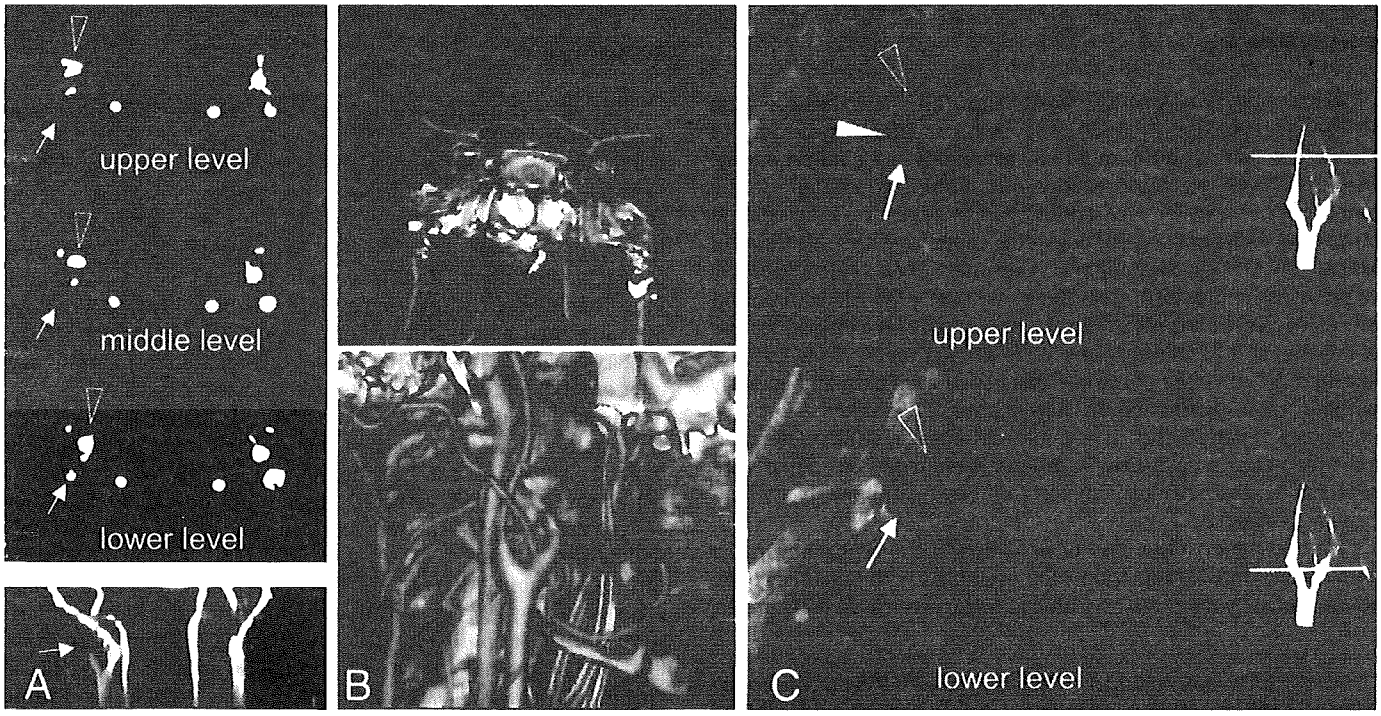

Fig. 2. MRI and 3D-CT angiography during the second stroke event. Cervical 3D-TOF MRA on admission of the second stroke shows right ICA occlusion distal to the carotid bifurcation (A). Source image did not show intramural hematoma or intimal flap. However, 3D-CT angiography on day 7showed reopening of the right MCA and ICA (B). The right ICA appears smooth and thin vessel without calcification. Black-blood MRI obtained on day 21 reveals neither intramural hematoma nor atherosclerotic plaque in the right ICA (C) (ICA, external carotid artery, and occipital artery are indicated by arrow, open arrowhead, and solid arrowhead, respectively).

One year later, at age 36, he was found unresponsive in the bathroom and transferred to this hospital. On admission, he was mute and unresponsive with profoundly decreased level of consciousness and left hemiparesis. Blood tests showed increased glucose level (9.60 mmol/L; HbA1c 7.7%) and elevated lactate level (1.96 mmol/L). Coagulation studies were normal. Carotid duplex sonography showed distal occlusion flow pattern in the right common carotid artery, but transaxial image of the internal carotid artery (ICA) was not obtained due to a high-positioned carotid bifurcation. DWI on admission (day 1) showed acute ischemic lesions in both MCA and anterior cerebral artery (ACA) territories (Fig. 1C). Apparent diffusion coefficient (ADC) values in the affected regions showed 49% reduction compared with those of the contralateral regions. Intracranial 3D-TOF MRA showed loss of signal of the right ICA and MCA, but distal A1 segment remained visible (Fig. 1D), suggesting right ICA, MCA, and proximal A1 occlusion. Cervical 3D-TOF MRA showed obliteration of the right ICA signal distal to the carotid bifurcation (Fig. 2A). Source images of MRA confirmed a lack of signal in expected location of the right ICA, but no intramural hematoma or intimal flap was seen. Blood flow SPECT revealed widespread hypoperfusion in right ICA territories.

After admission he received intravenous argatroban (anti-thrombin agent) for 7 days followed by intravenous heparin. He regained consciousness but left hemiparesis and mild aphasia remained. On day 7, 3D-CT angiography disclosed reopening of both right ICA and MCA (Fig. 2B). Cervical segment of the right ICA appeared smooth and thin without calcification. Conventional angiography on day 20 showed segmental narrowing of the right ICA and focal stenosis of the left ICA (Fig. 3C, D), but renal artery was not involved. Black-blood MRI, obtained using double inversion recovery with fat suppression to improve vessel-wall definition and minimize flow-related artifacts by suppressing blood, did not disclose atheromatous plaque or intramural hematoma in the right ICA, but rather thin artery without thickening of the wall (Fig. 2C), suggesting degenerative changes or developmental abnormality. Cardiac evaluation, including transesophageal echocardiography, was normal. CSF obtained 2 months after onset of second

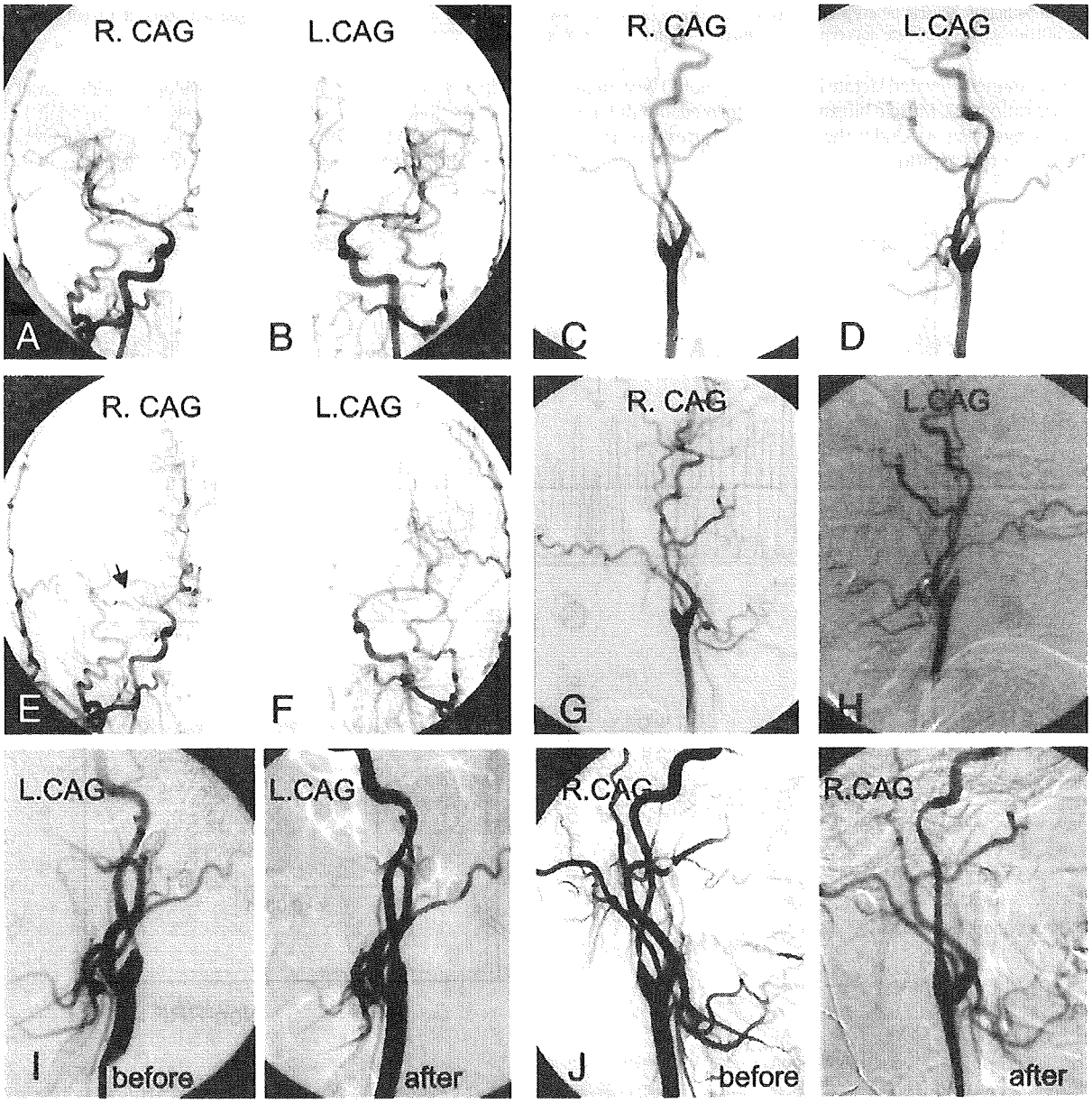

Fig. 3. Serial conventional angiography. Carotid angiography on day 20 of onset of the second stroke, at age 36, shows reopening of the MCA and ICA on the right side (see Figs. 1D and 2A), but segmental narrowing of the right ICA (C), and left carotid artery stenosis (D) are shown. Second angiography performed on day 11 of the onset of the third stroke, at age 37, shows a distal tapering occlusion of the right MCA M1 segment (E, arrow), and bilateral progressive carotid stenosis (G, H). Carotid angiography before and after carotid stent replacement is shown (I, J).

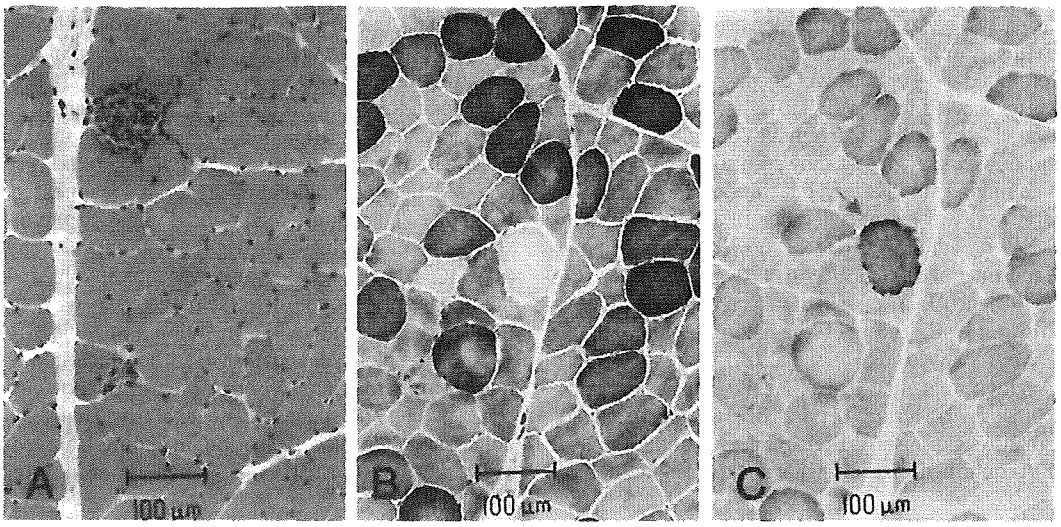

Fig. 4. Muscle histopathology. Muscle biopsy shows myopathic changes (A) with a few cytochrome *c* oxidase (COX)-negative ragged-red fibers (B, C), but strongly succinate dehydrogenase (SDH)-reactive vessels are not seen. (A; hematoxylin–eosin stain, B; COX stain, and C; SDH stain).

stroke showed sustained elevated lactate level (5.13 mmol/L) with high lactate/pyruvate ratio of 27. Muscle biopsy was performed, but did not show specific changes (Fig. 4). Under the diagnosis of artery-to artery embolism he was put on aspirin.

Fifteen months later, at age 37, he developed sudden onset of left leg weakness, followed by left arm weakness. On admission he had left hemiparesis. DWI on day 3 showed scattered cortico-subcortical lesions in the right MCA territories (Fig. 1E). 3D-TOF MRA showed loss of right

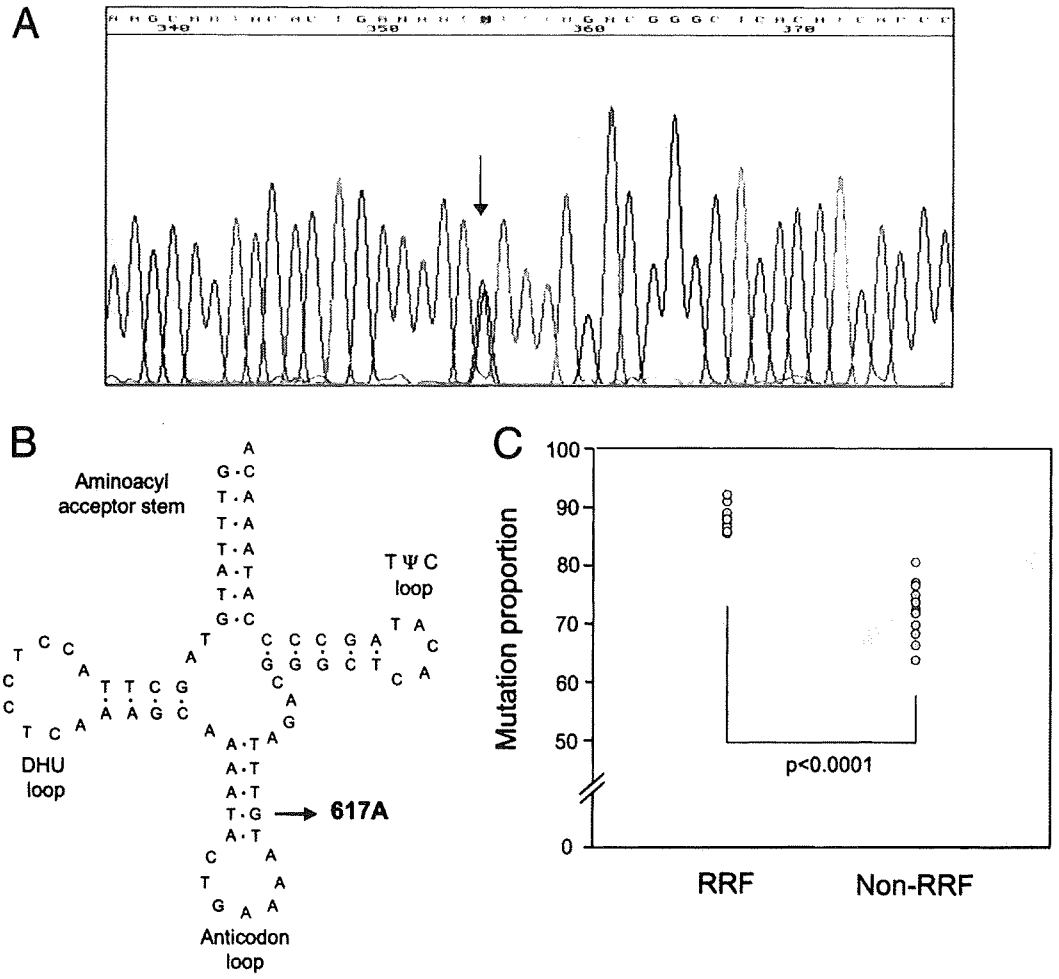

Fig. 5. Genetic analysis and single fiber analysis. Electropherograms demonstrate 50% heteroplasmic G617A transition (A, arrow). The location of the mutation is illustrated in schematic representation of the mitochondrial tRNA phenylalanine structure (B). Single muscle fiber analysis using a real-time PCR method shows significantly higher proportion of the G617A mutation in ragged-red fibers (RRF) than in non-RRF, confirming its pathogenicity (C). The *p* value is less than 0.0001 as calculated by the Mann–Whitney *U* test.

MCA signal (Fig. 1F). He received intravenous argatroban followed by warfarin, aspirin, and cilostazol. Conventional angiography on day 11 showed a tapering occlusion of the right MCA M1 segment, and progressive carotid artery stenosis on both sides (Fig. 3E–H). He underwent carotid artery stenting not carotid endarterectomy (Fig. 3I, J) because of high-positioned carotid bifurcation, absence of atherosclerotic plaque, and as-yet-unknown pathology in mitochondrial disorders. Carotid artery stent placement was performed using Wallstent RP (Boston Scientific) three months after presentation of the third stroke on the left (asymptomatic) side, followed by on the right side. During the first stent placement angiography revealed spontaneous resolution of the right MCA occlusion. Intravascular ultrasound image did not show plaque in the carotid artery. Although left carotid stent occlusion was incidentally found on subsequent follow-up angiography, no symptomatic ischemic stroke occurred for at least two years after surgery. He is currently able to walk with a cane and short leg brace.

3. Histopathological analysis

A biopsy specimen obtained from the left biceps brachii was processed for routine histochemical staining and immunostainings, including dsytrophin, sarcoglycan, dysferlin, caveolin 3, merosin, and collagen VI. Muscle biopsy showed myopathic changes with a few cytochrome *c* oxidase-negative ragged-red fibers (RRF), but strongly succinate dehydrogenase-reactive vessels were absent (Fig. 4). Some necrotic fibers were seen, but immunostainings were normal.

4. Genetic study

After informed consent from his family, genetic study was performed in this patient. DNA was isolated from blood by standard procedure, and direct sequencing of total mtDNA was performed. We applied the long PCR-based sequencing method to avoid nuclear pseudogene amplification. With 96 primer sets designed for sequencing, we obtained the reaction products using a big dye terminator cycle sequencing ready reaction kit (PE Applied Biosystems, USA), which were then analyzed with an ABI 3700 automated sequencer (PE Applied Biosystems, USA). Sequenced entire mtDNA was compared with a human mitochondrial genome database (MITOMAP; http://www.mitomap.org/).

Direct sequence revealed four mutations (E-table1), three of which were previously reported polymorphisms (G15323A, G15497A, A15860G), and one was a novel G617A transition in the mitochondrial tRNA phenylalanine gene (Fig. 5A, B). The transition was heteroplasmic (50%); not detected in 200 Japanese control subjects, not previously described in MITOMAP, and phylogenetically conserved (E-table2). Single muscle fiber analysis using a real-time PCR method [8] showed significantly higher proportion of the G617A mutation in RRF than in non-RRF (Fig. 5C). The mean G617A mutation rate was 74% in muscle specimen of the patient. After obtaining written informed consent, we also determined the G617A mutation rate in blood of his unaffected mother and brother who were normal on neurologic examination. It was 10.5% in each individual.

5. Discussion

This study provides three important implications in mitochondrial disorders. First, a novel G617A transition in the tRNA phenylalanine gene was identified in three members of this family examined and shown to be pathogenic in at least muscle pathology in this patient. Second, recurrent embolic strokes occur in mitochondrial disorders as macroangiopathy-related ischemic events. Third, progressive carotid artery stenosis could develop in mitochondrial disorders.

Regarding genetic study, at least 9 mutations in the tRNA phenylalanine gene [9–17] have been reported as pathogenic mutations of variable phenotypes including nephritis, [9] rhabdomyolysis, [10] progressive external ophthalmoplegia with deafness, [11] myoclonic epilepsy with ragged red fibers (MERRF), [12,13] and MELAS [14]. This novel G617A transition could also be pathogenic in this case because it is heteroplasmic; not described at MITOMAP; not found in 200 Japanese control subjects; and this codon is ubiquitously conserved. Single muscle fiber analysis confirmed its pathogenicity. The lack of symptoms in other members of this family can be explained by heteroplasmy of the mtDNA. However, it should be considered carefully whether these strokes are variant phenotypes of stroke-like episodes of MELAS, and this mutation has any causative role in involvement of major cervicocerebral arteries.

MELAS is usually defined by stroke-like episodes at a young age; encephalopathy characterized by seizures or progressive dementia or both; RRF on muscle biopsy; and lactic acidosis in CSF or blood or both [3]. Based on clinical grounds, one might consider MELAS in this case. However, in terms of symptomatology, neuroradiology, and electrophysiology, clinicoradiological features are different from those of stroke-like episodes of MELAS that we previously reported elsewhere [2,6,7]. MELAS patient often present with throbbing headache followed by seizure, visual symptoms or encephalopathy. Dysarthria or hemiparesis is not a presenting symptom. Seizure occasionally occurs during acute stage. Stroke-like lesions usually appear in the cortex incongruent to vascular territories with predilection to the posterior brain. Initial lesions may spread to adjacent cortex, often associated with prolonged focal epileptic activities. DWI reveals cortical hyperintense signal, but ADC values are usually normal or slightly increased or decreased. SPECT often shows focal hyperperfusion during acute stage. While this patient's three stroke events occurred in the cortex and/or subcortical regions in the MCA/ACA territories with a significant reduction in ADC values compatible with cytotoxic edema. These intracranial ischemic lesions appeared to be artery-to artery embolisms arising from carotid artery stenosis although no atherosclerotic plaque was demonstrated. MRA revealed transient occlusion of major cervicocerebral arteries. It is not appropriate to give a diagnosis of "MELAS" for this case.

Remarkable finding of this case is a major vessel stenosis. Cerebral arterial occlusion has been documented in only four cases of mitochondrial encephalomyopathy, [5,18–20] but carotid artery stenosis has never been reported yet. A 7-year-old girl was recently reported as an unusual case of MELAS with progressive cerebral vessel degeneration, [5] in which temporal occlusion of ICA was shown on 3D-TOF MRA, but no information about carotid stenosis or pathology of cerebral vessels was described. The etiology of carotid artery stenosis remains unknown, but atherosclerosis, arterial dissection or spasm is unlikely primary cause. Extracranial carotid artery fibromuscular dysplasia may cause high-grade stenosis, but neither "string of beads" sign nor renal artery involvement was demonstrated. Aortic rupture was reported in a case of MELAS harboring A3243G mutation as a phenotype of macroangiopathy, in which marked disarray of the smooth muscle architecture of the aorta was demonstrated [21]. Although we have not examined carotid artery pathologically, it could be possible to speculate that increased mutation load in the endothelium/smooth muscle cells may cause architectural changes in the carotid artery. Degenerative vascular changes distal to the carotid bifurcation that is most vulnerable to the shear stress may predispose this patient to developing artery-to artery embolism.

This case expands phenotypic spectrum of mitochondrial disorder, however, macroangiopathy-related ischemic events as reported here should be discriminated from classic stroke-like episodes that are believed to be microangioapthy-related events or neurovascular cellular events [2]. Cervicocerebral vascular degeneration can occur in mitochondrial encephalomyopathy, and treatment strategy should be determined based on pathophysiology.

Acknowledgments

The authors have nothing to disclose regarding funding, conflicts of interest or commercial relationships including grants, honoraria, speaker's lists, significant ownership, or financial support from pharmaceutical or other companies.

A part of this study was presented at the 5th International Congress on vascular dementia, held in Budapest, Hungary, November 8–11, 2007.

Appendix A. Supplementary data

Supplementary data associated with this article can be found, in the online version, at doi:10.1016/j.jns.2008.11.016.

References

[1] DiMauro S, Schon EA. Mitochondrial respiratory-chain diseases. N Engl J Med 2003;348:2656–68.
[2] Iizuka T, Sakai F. Pathogenesis of stroke-like episodes in MELAS: analysis of neurovascular cellular mechanisms. Curr Neurovasc Res 2005;2(1):29–45.
[3] Hirano M, Ricci E, Koenigsberger MR, Defendini R, Pavlakis SG, DeVivo DC, et al. MELAS: an original case and clinical criteria for diagnosis. Neuromuscul Disord 1992;2(2):125–35.
[4] Martínez-Fernández E, Gil-Peralta A, García-Lozano R, Chinchón I, Aguilera I, Fernández-López O, et al. Mitochondrial disease and stroke. Stroke 2001;32(11): 2507–10.
[5] Longo N, Schrijver I, Vogel H, Pique LM, Cowan TM, Pasquali M, et al. Progressive cerebral vascular degeneration with mitochondrial encephalopathy. Am J Med Genet A 2008;146(3):361–7.
[6] Iizuka T, Sakai F, Suzuki N, Hata T, Tsukahara S, Fukuda M, et al. Neuronal hyperexcitability in stroke-like episodes of MELAS syndrome. Neurology 2002;59 (6):816–24.
[7] Iizuka T, Sakai F, Kan S, Suzuki N. Slowly progressive spread of the stroke-like lesions in MELAS. Neurology 2003;61(9):1238–44.
[8] Komaki H, Akanuma J, Iwata H, Takahashi T, Mashima Y, Nonaka I, et al. A novel mtDNA C11777A mutation in Leigh syndrome. Mitochondrion 2003;2(4):293–304.
[9] Tzen CY, Tsai JD, Wu TY, Chen BF, Chen ML, Lin SP, et al. Tubulointerstitial nephritis associated with a novel mitochondrial point mutation. Kidney Int 2001;59(3): 846–54.
[10] Chinnery PF, Johnson MA, Taylor RW, Lightowlers RN, Turnbull DM. A novel mitochondrial tRNA phenylalanine mutation presenting with acute rhabdomyolysis. Ann Neurol 1997;41(3):408–10.
[11] Valente L, Piga D, Lamantea E, Carrara F, Uziel G, Cudia P, et al. Identification of novel mutations in five patients with mitochondrial encephalomyopathy. Biochim Biophys Acta 2008 Oct 15 [Electronic publication ahead of print].
[12] Ling J, Roy H, Qin D, Rubio MA, Alfonzo JD, Fredrick K, et al. Pathogenic mechanism of a human mitochondrial tRNAPhe mutation associated with myoclonic epilepsy with ragged red fibers syndrome. Proc Natl Acad Sci U S A 2007;104(39):15299–304.
[13] Mancuso M, Filosto M, Mootha VK, Rocchi A, Pistolesi S, Murri L, et al. A novel mitochondrial tRNAPhe mutation causes MERRF syndrome. Neurology 2004;62(11): 2119–21.
[14] Hanna MG, Nelson IP, Morgan-Hughes JA, Wood NW. MELAS: a new disease associated mitochondrial DNA mutation and evidence for further genetic heterogeneity. J Neurol Neurosurg Psychiatry 1998;65(4):512–7.
[15] Kleinle S, Schneider V, Moosmann P, Brandner S, Krahenbuhl S, Liechti-Gallati S. A novel mitochondrial tRNA(Phe) mutation inhibiting anticodon stem formation associated with a muscle disease. Biochem Biophys Res Commun 1998;247(1):112–5.
[16] Moslemi AR, Lindberg C, Toft J, Holme E, Kollberg G, Oldfors A. A novel mutation in the mitochondrial tRNA(Phe) gene associated with mitochondrial myopathy. Neuromuscul Disord 2004;14(1):46–50.
[17] Deschauer M, Swalwell H, Strauss M, Zierz S, Taylor RW. Novel mitochondrial transfer RNA(Phe) gene mutation associated with late-onset neuromuscular disease. Arch Neurol 2006;63(6):902–5.
[18] Destee A, Martin JJ, Muller JP, Scholte HR, Verier A, Largillière C, et al. Mitochondrial myopathy, encephalopathy with lactic acidosis and cerebral infarction. Central Rev Neurol 1989;145(1):37–48.
[19] Ito J, Tanaka H, Cho K, Kusunoki Y, Miyamoto A, Oki J. A patient with MELAS and arterial occlusive findings on cerebral angiography. J Child Neurol 1995;10(4):337–9.
[20] Noguchi A, Shoji Y, Matsumori M, Komatsu K, Takada G. Stroke-like episode involving a cerebral artery in a patient with MELAS. Pediatr Neurol 2005;33(1):70–1.
[21] Tay SH, Nordli DR, Bonilla E, Null E, Monaco S, Hirano M, et al. Aortic rupture in mitochondrial encephalopathy, lactic acidosis, and stroke-like episodes. Arch Neurol 2006;63(2):281–3.

Supplementary E-Table 1: Results of sequence of total mtDNA of the patient, and their frequency in the mitochondrial genome database (DB) obtained from 200 Japanese healthy subjects.

Region/gene	Change	Amino acid exchange	Frequency in DB	MITOMAP[1]
D-loop	a73g		98%	○
D-loop	c150t		14%	○
D-loop	a263g		83%	○
D-loop	ins-311c		85%	○
D-loop	g499a		3%	○
tRNA-Phe	g617a		0%	
12SrRNA	g709a		21%	○
12SrRNA	a750g		99%	○
12SrRNA	a827g		3%	○
12SrRNA	a1438g		92%	○
16SrRNA	a2706g		99%	○
ND1	a3714g	syn	0%	○
ND2	a4769g	syn	99%	○
ND2	a4793g	syn	3%	○
ND2	a4833g	T-A	6%	○
ND2	t5108c	syn	9%	○
CO I	c7028t	syn	99%	○
CO II	c7867t	syn	3%	○
CO II	t8200c	syn	1%	○
ATP6	a8701g	T-A	45%	○
ATP6	a8860g	T-A	100%	○
CO III	t9540c	syn	52%	○
ND3	a10398g	T-A	70%	○
ND3	c10400t	syn	63%	○
ND4	t10873c	syn	63%	○
ND4	a11084g	T-A	6%	○
ND4	g11719a	syn	100%	○
ND4	g11914a	syn	8%	○
ND5	c12705t	syn	73%	○
ND6	g14569a	syn	7%	○
cyt b	c14766t	I-T	100%	○
cyt b	t14783c	syn	65%	○
cyt b	g15043a	syn	63%	○
cyt b	g15301a	T-A	49%	○
cyt b	g15323a	T-A	4%	
cyt b	a15326g	T-A	99%	○
cyt b	c15535t	syn	1%	○
cyt b	g15497a	G-S	3%	
cyt b	a15860g	I-V	1%	
D-loop	c16223t		75%	○
D-loop	t16325c		5%	○
D-loop	t16362c		43%	○
D-loop	t16519c		58%	○

Four mutations are found, three of which (G15323A, G15497A, A15860G) were previously reported polymorphisms. G617A substitution in the mitochondrial $tRNA^{phe}$ gene is found to be heteroplasmic of 50% (see figure 5A).

Reference:

1. MITOMAP: A Human Mitochondrial Genome Database. http://www.mitomap.org, 2008.

A Loss-of-Function Mutation in the *FTSJ1* Gene Causes Nonsyndromic X-Linked Mental Retardation in a Japanese Family

Kyoko Takano,[1] Eiji Nakagawa,[1] Ken Inoue,[1] Fumiaki Kamada,[2] Shigeo Kure,[2] Yu-ichi Goto,[1]* and Japanese Mental Retardation Consortium

[1]*Department of Mental Retardation and Birth Defect Research, National Institute of Neuroscience, National Center of Neurology and Psychiatry, Tokyo, Japan*
[2]*Department of Medical Genetics, Tohoku University School of Medicine, Sendai, Japan*

Mental retardation (MR) is a common trait, affecting ~2–3% of individuals in the general population. Although the etiology of MR remains largely unknown, genetics apparently play a major role. Recent molecular studies of X-linked form of MR in European and North American countries have revealed 24 nonsyndromic X-linked mental retardation (NS-XLMR) genes including *FTSJ1*, a human homolog of the *Escherichia coli* 2′-*O*-rRNA methyltransferase FtsJ/RrmJ gene. Here we identified a novel *FTSJ1* mutation in an XLMR family through mutation screening of a cohort of 73 unrelated Japanese male probands with MR. Sequence analysis of the proband and his mother revealed a G > A substitution at the consensus for the donor splicing site in intron 8 (c.571 + 1G > A) of *FTSJ1*. This mutation prevented the removal intron 8 from the pre-mRNA, thereby leading to a frameshift in the mutant *FTSJ1* mRNA and resulting in a premature termination in exon 9. Quantitative RT-PCR showed a significant reduction of mutant *FTSJ1* mRNA in the patient's lymphoblast cells, which was restored by treatment with cycloheximide, a potent inhibitor of nonsense-mediated mRNA decay (NMD). Therefore, mRNAs carrying this mutation are likely subject to degradation by NMD. Together, loss-of-function of *FTSJ1* may be a mechanism for the cognitive dysfunction observed in this family. Our study also suggested that the *FTSJ1* mutation probably accounts for XLMR in Japanese at a similar frequency (1–2%) as in Europeans. © 2007 Wiley-Liss, Inc.

KEY WORDS: splice site mutation; nonsense-mediated mRNA decay; premature termination codon; mutation frequency

Please cite this article as follows: Takano K, Nakagawa E, Inoue K, Kamada F, Kure S, Goto Y-i. 2008. A Loss-of-Function Mutation in the *FTSJ1* Gene Causes Nonsyndromic X-Linked Mental Retardation in a Japanese Family. Am J Med Genet Part B 147B:479–484.

INTRODUCTION

Mental retardation (MR) is one of the most frequent developmental disorders in children, and its prevalence is thought to be 2–3% in the general population [Chelly and Mandel, 2001; Leonard and Wen, 2002]. Similarly, the estimated prevalence of MR in Japanese children from 3 to 12 years old is 0.6–1.3% [Kaga et al., 2002]. Etiology of MR is genetically and environmentally heterogeneous. Of the genetic factors, X-linked genes appear to be important contributors to MR, as reflected by the higher frequency of MR in male than female [Ropers and Hamel, 2005]. The prevalence of X-linked mental retardation (XLMR) in male MR patients was estimated to be 10% [Ropers and Hamel, 2005]. XLMR is classified into nonsyndromic and syndromic XLMR (NS-XLMR and S-XLMR, respectively) [Ropers and Hamel, 2005]. NS-XLMR presents with only intellectual impairment, whereas S-XLMR shows additional symptoms such as craniofacial anomaly, brain malformation, and/or metabolic abnormality. NS-XLMR

Yu-ichi Goto, Department of Mental Retardation and Birth Defect Research, National Institute of Neuroscience, National Center of Neurology and Psychiatry, Tokyo, Japan; Johji Inazawa, Department of Molecular Cytogenetics, Medical Research Institute and School of Biomedical Science, Tokyo Medical and Dental University, Tokyo, Japan; Mitsuhiro Kato, Department of Pediatrics, Yamagata University School of Medicine, Yamagata, Japan; Takeo Kubota, Department of Epigenetic Medicine, Interdisciplinary Graduate School of Medicine and Engineering, University of Yamanashi, Yamanashi, Japan; Kenji Kurosawa, Division of Medical Genetics, Kanagawa Children's Medical Center, Yokohama, Japan; Naomichi Matsumoto, Department of Human Genetics, Yokohama City University Graduate School of Medicine, Yokohama, Japan; Eiji Nakagawa, Department of Mental Retardation and Birth Defect Research, National Institute of Neuroscience, National Center of Neurology and Psychiatry, Tokyo, Japan; Eiji Nanba, Division of Functional Genomics, Research Center for Bioscience and Technology, Tottori University, Yonago, Japan; Hitoshi Okazawa, Department of Neuropathology, Medical Research Institute and 21st Century Center of Excellence Program for Brain Integration and Its Disorders, Tokyo Medical and Dental University, Tokyo, Japan; Shinji Saitoh, Department of Pediatrics, Hokkaido University Graduate School of Medicine, Sapporo, Japan; Takahito Wada, Department of Medical Genetics, Shinshu University School of Medicine, Matsumoto, Japan.

Grant sponsor: Ministry of Health, Labour and Welfare, Japan; Grant numbers: 15B-4, 18A-5; Grant sponsor: Japan Society for the Promotion of Science, Japan; Grant number: 1739012.

*Correspondence to: Yu-ichi Goto, M.D., Ph.D., Department of Mental Retardation and Birth Defect Research, National Institute of Neuroscience, National Center of Neurology and Psychiatry, 4-1-1 Ogawahigashi, Kodaira, Tokyo 187-8502, Japan.
E-mail: goto@ncnp.go.jp

Received 28 February 2007; Accepted 31 August 2007
DOI 10.1002/ajmg.b.30638

accounts for two thirds of XLMR [Fishburn et al., 1983]. At present, a total of 61 genes have been associated with XLMR, 24 of which are associated with NS-XLMR by molecular studies conducted in Europe and North America [Ropers, 2006]. In Japan, we have organized an MR research consortium and have been developing a research resource repository since 2003. Genomic DNA, lymphoblast cells and clinical information obtained from 73 families with MR (44 familial and 29 sporadic cases) have been collected and registered at the National Center of Neurology and Psychiatry, Tokyo, as of September 2006. As a part of our search for genetic abnormalities using this patient cohort, we identified a mutation in *FTSJ1* in a large Japanese family with NS-XLMR. This mutation resulted in a downregulation of *FTSJ1* mRNA expression. Therefore, loss-of-function is the likely molecular mechanism underlying the cognitive dysfunction in this family.

MATERIALS AND METHODS

Patients

Seventy-three Japanese male patients with MR were subjected to the screening of *FTSJ1* mutation. Forty-four were familial, with at least two mentally retarded individuals and 29 were sporadic. Peripheral blood samples were obtained with informed consent approved by the Institutional Review Board, National Center of Neurology and Psychiatry. Expansion of *FMR1*, the common mutation for fragile X syndrome, was excluded by PCR assay [Nanba et al., 1995].

Clinical Findings of MRW06 Family

The family MRW06 was referred for genetic counseling. The family has six affected males with nonsyndromic mental retardation consistent with X-linked recessive inheritance (Fig. 1). The index patient (IV-7) who is now 14 years old was referred for moderate MR. Parents were non-consanguineous. Maternal pregnancy and delivery were uneventful. He acquired head control at 4 months, crawling at 12 months, and walking unassisted at 18 months. His MR was first evaluated clinically at 3 years old, because of his delayed speech. He attended special school at 7 years old. His full-scale IQ was 37 at 12 years old. He experienced an episode of febrile seizure at 3 years old, but had no attack since then. On recent clinical examination at 14 years old, his height was 168.5 cm (75th percentile), his weight was 55.3 kg, and his head circumference was 56.5 cm (50th to 75th percentile). He had no dysmorphic or neurologic abnormalities. His electroencephalogram showed sporadic epileptic discharges around the centro-parietal area in sleep record. His cranial computed tomography was normal at 10 years old. Currently, he can have a simple conversation and can write his name and numerals. He apparently shows behavior problems such as obsessive-compulsive, stereotypy, aggressive, outburst, mild self-injury, and panic symptoms. He needs to take haloperidol, fluvoxamine, and carbamazepine to control these problems.

His mother (III-9) is a healthy carrier with normal intelligence. His 57-year-old maternal uncle (III-7) has mild MR. The uncle used to work at a laundry to support himself, but currently lives in a group home. He shows mild behavioral problems including obsessiveness. Although the detailed clinical records of four other affected males were not available, the history of each individual obtained from the index family strongly suggested that these individuals have MR.

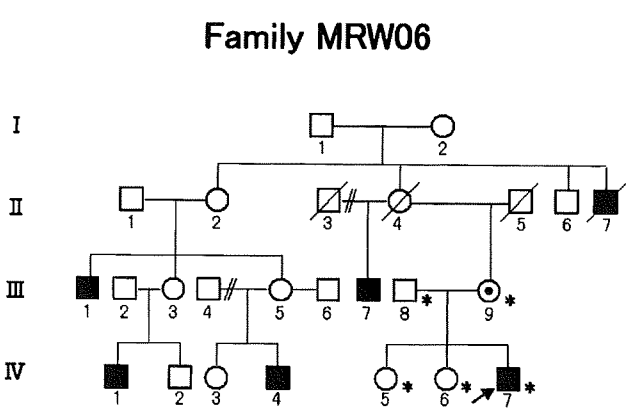

Fig. 1. Pedigree of MRW06 family. Arrow indicates the index patient. Asterisks indicate family members tested for the mutation. Closed squares and a dotted circle show affected males and a carrier female, respectively.

Cell Culture

Epstein–Barr Virus (EBV)-transformed lymphoblast cells were established from peripheral blood cells using the standard methods [Darlington, 1998]. All lymphoblast cells were cultured in RPMI 1640 medium supplemented with 10% fetal bovine serum and antibiotics. To prevent potential degradation of transcripts containing premature termination codons (PTCs) by nonsense-mediated mRNA decay (NMD), lymphoblast cells from the patient, the mother and normal controls were treated with 100 μg/ml cycloheximide (CHX) (Sigma, St. Louis, MO) or with 0.1% DMSO as vehicle control, 4 hr prior to the RNA extraction [Carter et al., 1995].

Mutation Analysis of *FTSJ1* Gene

Genomic DNA from EBV-transformed lymphoblast cells was isolated using PUREGENE DNA purification Kit (Gentra systems, Minneapolis, MN). Eleven coding exons of *FTSJ1* were amplified by PCR using primers described elsewhere [Freude et al., 2004]. PCR products purified, by Montage $PCR_{\mu 96}$ Plate (MILLIPORE, Billerica, MA), were directly sequenced using the BigDye Terminator v1.1 chemistry and ABI 3700 DNA analyzer (Applied Biosystems, Foster City, CA). We verified the frequency of the alterations by examination of control genomic DNA from 48 Japanese males and 47 females. PCR products from exon 8 were digested with *Cla* I, followed by electrophoretic separation in a 3% agarose gel and visualization by ethidium bromide staining.

RT-PCR

Total RNA from cultured lymphoblast cells from the patient, parents and normal controls were extracted using RNeasy Mini kit (QIAGEN, Germany), and were converted to cDNA using SuperScript III reverse transcriptase and Random primers (Invitrogen, Carlsbad, CA). The entire coding sequence of *FTSJ1* (exons 2–12) was amplified by PCR using a pair of flanking primers [Ramser et al., 2004], and sequenced after gel isolation and purification or subcloning into pCR 2.1-TOPO vector (Invitrogen). To verify whether two aberrant transcripts also exist in normal controls, RT-PCR analysis was done on the patient and normal controls using primer pairs designed to specifically amplify them. Each pair was designed for amplifying introns 8–11 and exons 3–13, respectively (primer sequences and PCR condition available on request).

Real-Time Quantification of *FTSJ1* mRNA

We used the comparative standard curve method (relative standard curve) with SYBRGreen. Primers were designed with Primer Express software (Applied Biosystems), as follows: forward primer in exon 2; 5′-AAACTGCTACAACTGGATAAGGAATTC-3′ and reverse primer in exon 3; 5′-GGGCTGCACA-

CAGGTCAACT-3′. We used primer sets for *GAPDH* and *ACTB* as internal controls [Murphy et al., 2003]. For relative quantification, the reaction mixtures consisted of *Power* SYBR Green PCR Master Mix (Applied Biosystems), with 1 μM of each primer and cDNA generated from 1.25 ng total RNA in a total volume of 10 μl. After an initial denature step for 10 min at 95°C, thermal cycling condition was 15 sec at 95°C and 1 min at 60°C for 40 cycles. Finally, the dissociation curve for each reaction was determined to validate the specificity of the amplification. All samples were run in triplicate on an ABI PRISM 7900 instrument, and two independent runs were performed for all samples.

X Chromosome Inactivation Study

The androgen receptor (*AR*) X chromosome inactivation (XCI) study was done using a PCR-based assay with slight modifications [Allen et al., 1992]. Genomic DNA (1 μg) extracted from peripheral leukocytes and lymphoblast cells was digested with methylation-sensitive restriction enzyme *Hpa II* in a total volume of 10 μl. Then, 1 μl of the digested DNA was amplified by PCR using a pair of 6-carboxyfluorescein (FAM)-labeled primers flanking the restriction site and a polymorphic CAG repeat, which results in amplification of alleles on the inactive X chromosome only. In females who are heterozygous for the *AR* polymorphism, 2 PCR products can be separated. Next, 1 μl of PCR products with 10 μl Hi-Di Formamide and 0.1 μl GeneScan-500 LIZ Size Standard were run on an ABI 3130 genetic analyzer, and peak areas were calculated by GeneMapper software (Applied Biosystems). The raw peak area value of the digested samples was corrected for amplification efficiency using data from undigested samples. Each sample was assessed in two independent reactions.

RESULTS

Splice Site Mutation in the *FTSJ1* Gene

Sequence analysis of the proband revealed a G-to-A substitution at the consensus for the donor splicing site in intron 8 (c.571 + 1G > A) of the *FTSJ1* gene (Fig. 2). His mother was found to be a carrier of this mutation, which was absent in his father and two healthy sisters. A polymorphism study showed that this mutation was not present in 142 normal X chromosomes (48 males and 47 females) from a Japanese population. No further *FTSJ1* mutation was identified in the other 72 MR patients except for a common polymorphism in intron 8 (rs2070991).

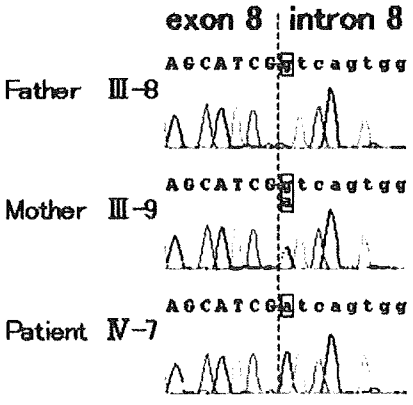

Fig. 2. Chromatograms from genomic sequencing analysis showing exon 8 to intron 8 boundary. Rectangles indicate the position c.571 + 1. Patient (IV-7) showed a G-to-A substitution at the consensus for the donor splicing site in intron 8 (c.571 + 1G > A). Mother (III-9) was heterozygous for this mutation.

c.571 + 1G > A Mutation Resulting in Aberrant Splicing

The effect of the c.571 + 1G > A splice site mutation was determined by analyzing the *FTSJ1* transcripts obtained from lymphoblast cells (Fig. 3). The major transcript that contains putative coding region (exons 2–12) from the patient was apparently longer (1,293 bp) than that obtained from control individuals (1,190 bp). The mother showed only a single band of normal length. Nucleotide sequencing of the patient's major transcript revealed retention of the entire intron 8, which conceptually leads to a frameshift in the *FTSJ1* mRNA and results in a premature termination codon (PTC) at position 597 in exon 9 (Fig. 4). Additional faint longer bands were detected in the patient's sample (Fig. 3). Sequencing analysis of subcloned inserts showed two aberrant transcripts, one retaining introns 8 and 11 (1,484 bp) and the other missing exons 6–12 (552 bp). However, both of these transcripts were also detected in control samples by RT-PCR using primers designed to specifically amplify them (not shown). Therefore, these transcripts probably represent normally existing minor alleles.

Significant Decrease of Mutant *FTSJ1* mRNA by NMD Activation

To investigate whether this splice site mutation can affect the expression level of the *FTSJ1* gene, we measured the *FTSJ1* mRNA level in the patient's and his parents' cells by real-time quantitative RT-PCR (qRT-PCR). The mother is a heterozygous carrier for the mutation, while the father can serve as a normal male control. Primers were designed to amplify both mutant and wild type alleles with equal efficiency (Fig. 4B). The patient showed a significant reduction of *FTSJ1* mRNA in comparison with both parents (Fig. 5).

We next determined whether the dramatic decrease of the *FTSJ1* mRNA in the patient was mediated by NMD, an mRNA surveillance system that selectively detects and degrades mRNAs carrying PTCs [Holbrook et al., 2004; Inoue et al., 2004; Maquat, 2004; Wilkinson, 2005], because the mutant *FTSJ1* transcripts contain PTC in exon 9 and presumably become substrates for NMD. We treated the lymphoblast cells with CHX, a translation inhibitor that can mitigate the effect of NMD [Carter et al., 1995; Noensie and Dietz, 2001], followed by RNA isolation and real-time quantification. Treatment of the patient's lymphoblast cells with CHX resulted in a threefold increase of *FTSJ1* transcript (Fig. 6). Smaller increases of *FTSJ1* transcript observed in the mother and the normal controls were not statistically significant.

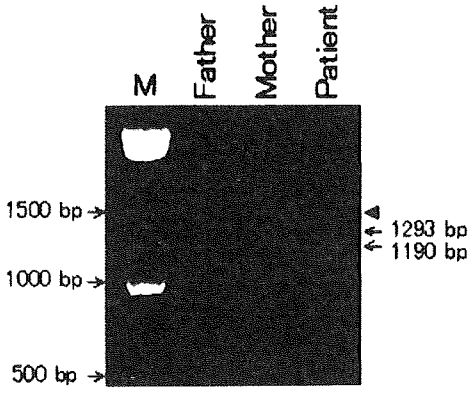

Fig. 3. RT-PCR amplification of the *FTSJ1* gene encompassing exon 2 to exon 13. The patient (IV-7) showed a 1,293 bp product, which was longer than wild-type, as defined by subsequent DNA sequencing analysis. Additional faint bands were also observed in the patient's sample as indicated by arrowhead. M, 100 bp ladder (Roche, Switzerland).

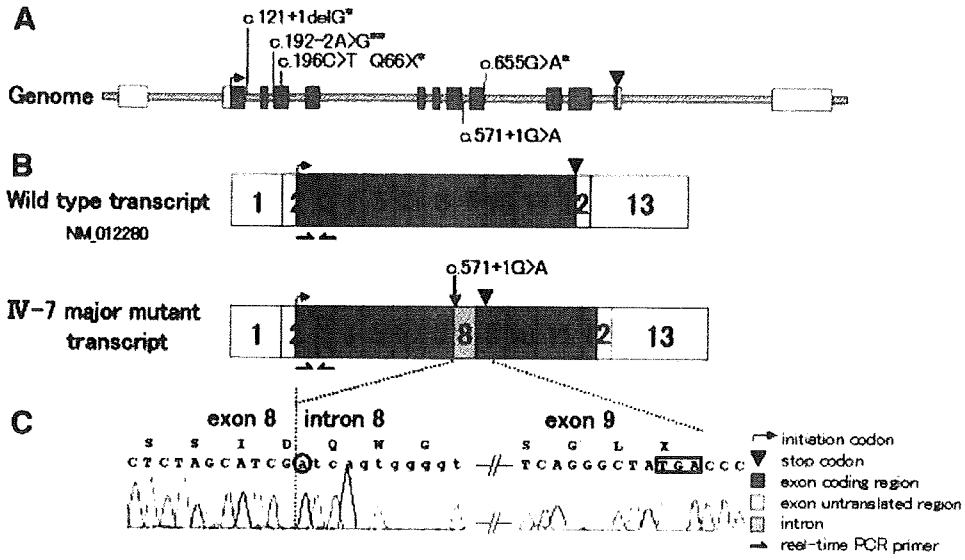

Fig. 4. Sequencing analysis of major mutant transcript from the patient. **A**: Genomic structure of the *FTSJ1* gene. Mutations reported previously are shown above (*Freude et al., **Ramser et al.) and the mutation found in this study is shown below. **B**: A comparison of wild type and mutant *FTSJ1* mRNA structures, (**C**); Partial sequence chromatogram of mutant cDNA obtained from the patient. c.571 + 1G > A mutation is marked by a circle, and the putative premature termination codon in exon 9 is shown in a rectangle.

Preferentially Skewed X Chromosome Inactivation in the Mother

To determine the molecular basis for the monoallelic expression of normal *FTSJ1* in the mother, we performed XCI study of *AR* locus (Fig. 7). The mother showed a skewed XCI pattern in both peripheral leukocytes (97:3) (Fig. 7) and lymphoblast cells (99:1) (not shown), whereas the patient's two noncarrier sisters both showed random XCI pattern (76:24 and 59:41) in peripheral leukocytes (Fig. 7). It is likely that the inactive X chromosome harbors the mutant allele in the mother, considering the relatively small genetic distance between *AR* and *FTSJ1* (>5 centimorgan by the Genethon genetic map, NCBI Map Viewer, http://www.ncbi.nlm.nih.gov/mapview/) and the lack of haplotypic evidence that supports recombination within this pedigree (Fig. 7). Although XCI in the central nervous system has not been determined, these findings suggest that the expression of *FTSJ1* mutant allele was suppressed in the mother predominantly because of skewed X inactivation, rather than post-transcriptional mRNA degradation by NMD.

DISCUSSION

Through screening of the *FTSJ1* gene using a cohort of 73 Japanese individuals with MR, we identified a novel splice site mutation (c.571 + 1G > A) in a family with NS-XLMR. Because all four *FTSJ1* mutations reported previously were found in European NS-XLMR families, this is the first *FTSJ1* mutation identified in non-European family. The prevalence of *FTSJ1* mutation in families with NS-XLMR was estimated as 1–2% in

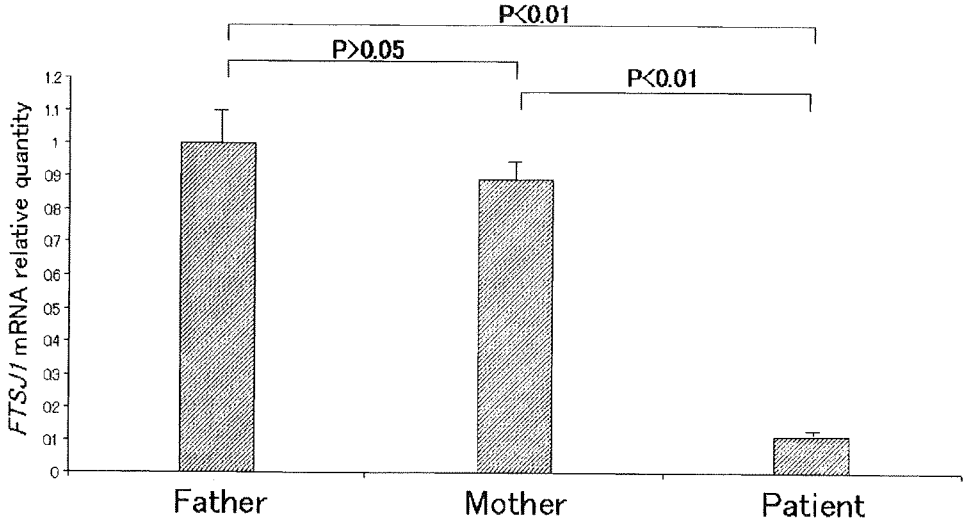

Fig. 5. Real-time quantification of *FTSJ1* mRNA in the patient and his parents. The quantitation of *FTSJ1* mRNA was normalized to *GAPDH* mRNA, with the level in the father referred to as 1. The amount of *FTSJ1* mRNA in the patient's lymphoblast cells was 10 times smaller than that of his father, which served as a control. Representative data from two independent experiments, each run in triplicate, were shown. Statistical analyses were performed using Student's *t*-test. Bars indicate means + SD.